Euscorpius

Occasional Publications in Scorpiology

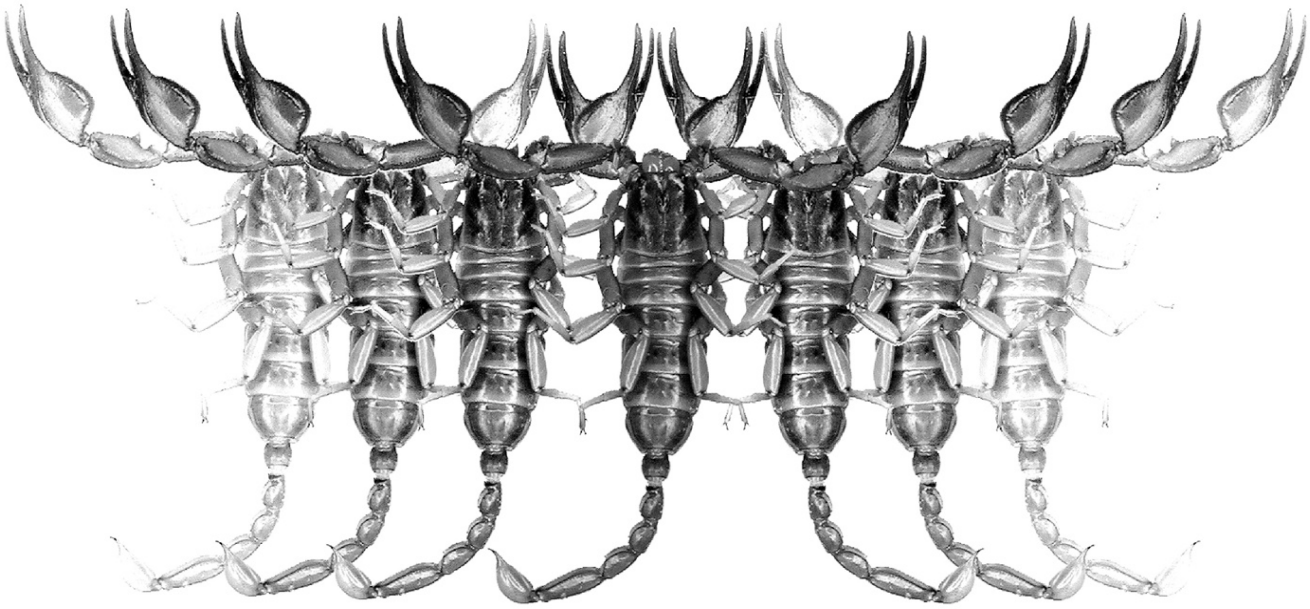

Trypanothacus gen. n., a new genus of burrowing scorpion from the Arabian Peninsula (Scorpiones: Buthidae)

Graeme Lowe, František Kovařík, Mark Stockmann & František Šťáhlavský

February 2019 — No. 277

Euscorpius

Occasional Publications in Scorpiology

EDITOR: **Victor Fet**, Marshall University, **'fet@marshall.edu'**

ASSOCIATE EDITOR: **Michael E. Soleglad, 'msoleglad@gmail.com'**

Euscorpius is the first research publication completely devoted to scorpions (Arachnida: Scorpiones). ***Euscorpius*** takes advantage of the rapidly evolving medium of quick online publication, at the same time maintaining high research standards for the burgeoning field of scorpion science (scorpiology). ***Euscorpius*** is an expedient and viable medium for the publication of serious papers in scorpiology, including (but not limited to): systematics, evolution, ecology, biogeography, and general biology of scorpions. Review papers, descriptions of new taxa, faunistic surveys, lists of museum collections, and book reviews are welcome.

Derivatio Nominis

The name ***Euscorpius*** Thorell, 1876 refers to the most common genus of scorpions in the Mediterranean region and southern Europe (family Euscorpiidae).

Euscorpius is located at: https://mds.marshall.edu/euscorpius/
Archive of issues 1-270 see also at: http://www.science.marshall.edu/fet/Euscorpius

(Marshall University, Huntington, West Virginia 25755-2510, USA)

ICZN COMPLIANCE OF ELECTRONIC PUBLICATIONS:

Electronic ("e-only") publications are fully compliant with ICZN (*International Code of Zoological Nomenclature*) (i.e. for the purposes of new names and new nomenclatural acts) when properly archived and registered. All ***Euscorpius*** issues starting from No. 156 (2013) are archived in two electronic archives:

- **Biotaxa,** http://biotaxa.org/Euscorpius (ICZN-approved and ZooBank-enabled)
- **Marshall Digital Scholar**, http://mds.marshall.edu/euscorpius/. (This website also archives all *Euscorpius* issues previously published on CD-ROMs.)

Between 2000 and 2013, ICZN ***did not accept online texts*** as "published work" (Article 9.8). At this time, *Euscorpius* was produced in two ***identical*** versions: online (*ISSN 1536-9307*) and CD-ROM (*ISSN 1536-9293*) (laser disk) in archive-quality, read-only format. Both versions had the identical date of publication, as well as identical page and figure numbers. ***Only copies distributed on a CD-ROM*** from ***Euscorpius*** in 2001-2012 represent published work in compliance with the ICZN, i.e. for the purposes of new names and new nomenclatural acts.

In September 2012, ICZN Article 8. What constitutes published work**,** has been amended and allowed for electronic publications, disallowing publication on optical discs. From January 2013, ***Euscorpius*** discontinued CD-ROM production; only online electronic version (ISSN 1536-9307) is published. For further details on the new ICZN amendment, see http://www.pensoft.net/journals/zookeys/article/3944/.

Publication date: 19 February 2019

http://zoobank.org/urn:lsid:zoobank.org:pub:64451868-1FB3-4D20-B88D-FBF7304EB775

Euscorpius — Occasional Publications in Scorpiology. 2019, No. 277

Trypanothacus gen. n., a new genus of burrowing scorpion from the Arabian Peninsula (Scorpiones: Buthidae)

Graeme Lowe [1], František Kovařík [2,4], Mark Stockmann[3] & František Šťáhlavský [4]

[1] Monell Chemical Senses Center, 3500 Market St., Philadelphia, PA 19104-3308, USA
[2] P.O. Box 27, CZ - 145 01 Praha 45, Czech Republic; http://www.scorpio.cz
[3] Im Hoek 20, D-48477 Hörstel-Riesenbeck, Germany
[4] Department of Zoology, Charles University, Viničná 7, CZ-128 44 Praha 2, Czech Republic

http://zoobank.org/urn:lsid:zoobank.org:pub:64451868-1FB3-4D20-B88D-FBF7304EB775

Summary

We define a new fossorial buthid genus *Trypanothacus* **gen**. **n**., similar to *Buthacus* Birula, 1908, differing primarily in telson shape, with a bulbous vesicle and aculeus shorter than the vesicle, and in heavier dentition on metasomal segments II–III and IV. The new genus includes two species: *T. barnesi* **sp**. **n**. from Oman and *T. buettikeri* (Hendrixson, 2006) **comb**. **n**. from Saudi Arabia, the latter transferred from *Buthacus*. We provide detailed illustrations of both species from preserved materials, and in vivo habitus and natural habitat are shown for *T. barnesi* **sp**. **n**.. Information is also provided on ecology and captive rearing of *T. barnesi* **sp. n.**, and on its karyotype (2n=26). The new genus is compared to genera *Buthacus* and *Vachoniolus* Levy et al., 1973. Telson morphology of these genera is analyzed and compared with other psammophilous and pelophilous buthids. In certain subgroups of scorpions, we find that aculeus length can be related to psammophily and body size. As a highly diverse multifunctional organ, the telson is shaped by complex environmental and genetic factors. We propose that telson morphology can nevertheless be useful for taxonomy if it is carefully applied.

Introduction

The genus *Buthacus* (Birula, 1908) embraces a heterogeneous assemblage of psammophile scorpions in the 'Buthus group', a large Palaearctic buthid clade distributed widely across North Africa, the Middle East and Asia (Fet et al., 2005). *Buthacus* has a lengthy and convoluted taxonomic history. Current composition of the genus and validity of some species are still vigorously debated. Kovařík (2005) examined and revised types of early species and critically reviewed others. Lourenço (2006) again revised the genus and expressed opposing opinions on the validity of some species. Over the years, new species were individually added, while others were shuffled in or out of synonymy (e.g., Lourenço, 2006; Lourenço & Qi, 2006; Lourenço & Leguin 2009; Kovařík et al., 2016b; Kovařík, 2018). However, beyond nomenclatural issues at the species level, a broader effort is needed to understand and clarify the scope of the genus. In its current state, the genus may be paraphyletic or polyphyletic because species sorted into *Buthacus* share some probably primitive characters, while other similarities may reflect convergent arenicolous adaptation.

Kovařík et al. (2013) made progress towards addressing this problem by establishing the Horn of Africa genus *Gint*, for *Buthus calviceps* Pocock, 1900, a species previously assigned to *Buthacus*, and for *Gint gaitako* Kovařík et al., 2013. To differentiate *Buthacus*, they revised its generic diagnosis to include additional new characters: carapace with polished preocular area; distinctive telson shape, with pyriform vesicle and long curved aculeus (that equals or exceeds the vesicle in length); and higher number of granule rows (9–12) on the dentate margin of the pedipalp movable finger.

Here, we continue to refine the taxonomy of *Buthacus* by splitting off another new genus, *Trypanothacus* **gen**. **n**., that includes another species previously described under *Buthacus*, i.e. *B*. *buettikeri* Hendrixson, 2006, from Saudi Arabia. As already mentioned in prior publications, *B*. *buettikeri* does not fit the revised diagnosis of *Buthacus*, specifically in the shape of the telson (cf. Kovařík et al., 2013; Kovařík et al., 2016b; Kovařík, 2018). We also describe under the new genus a new species *T*. *barnesi* **sp**. **n**., endemic to central and southern Oman. We discuss other species that could be candidates for membership in the new genus. We analyze trends in telson morphology of *Buthacus*, *Trypanothacus* **gen**. **n**., *Vachoniolus* Levy et al., 1973, and other psammophile and ultrapsammophile 'Buthus group' species, comparing them to other burrowing buthids. We suggest some ecological factors that may underlie these trends.

Methods, Material & Abbreviations

General laboratory methods follow Sissom et al. (1990). Nomenclature and measurements follow Stahnke (1971), Kovařík (2009), and Kovařík & Ojanguren Affilastro (2013), except for trichobothriotaxy (Vachon, 1974). Hemispermatophore methods and terminology follow

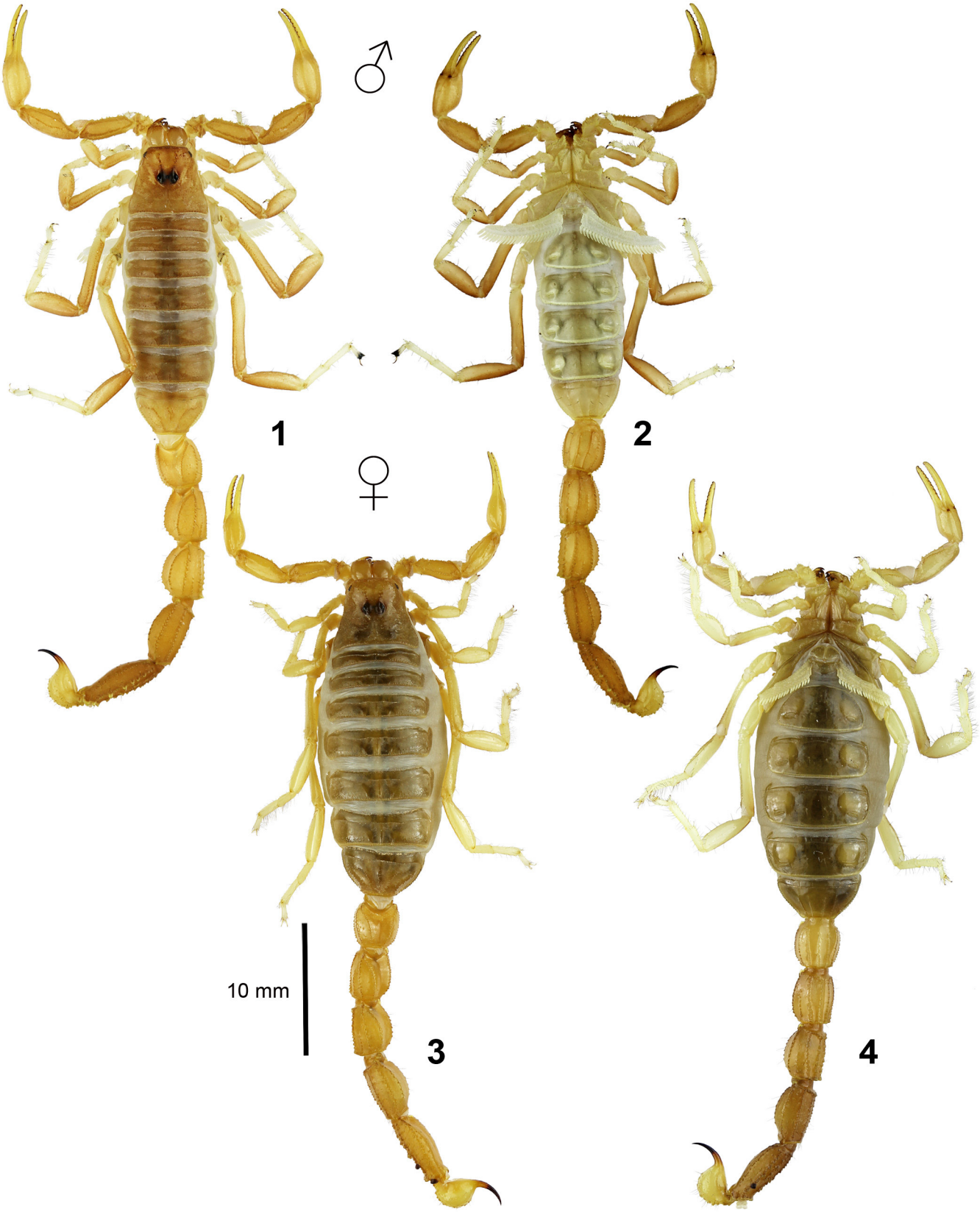

Figures 1–4: *Trypanothacus barnesi* **gen**. et **sp**. **n**. **Figures 1–2**. Male paratype from the type locality in dorsal (1) and ventral (2) views. **Figures 3–4**: Female paratype from the type locality in dorsal (3) and ventral (4) views. Scale bar: 10 mm.

Kovařík et al. (2018). White light and UV imaging methods follow Lowe et al. (2014) and Lowe (2018). Biometric or karyotype analyses utilized software Image J 1.44p/ 1.45r (http://rsbweb.nih.gov/ij), Origin 7.0 (https://www.originlab.com) and Microsoft Excel 2010. Coordinates of localities in Saudi Arabia collected by W. Büttiker were obtained from published gazetteers in Ahrens (2000) and Lewis & Büttiker (1982) (cited in square brackets). *Specimen Depositories*: FKCP (František Kovařík, private collection, Prague, Czech Republic); GLPC (Graeme Lowe, private collection, Philadelphia, USA); NHMB (Naturhistorisches Museum Basel, Switzerland); MNHN (Muséum National d'Histoire Naturelle, Paris, France); ONHM (Oman Natural History Museum, Muscat, Oman). *Morphometrics*: D, depth; L, length; W, width. *Statistics:* sd, standard deviation; sem, standard error of the mean.

Systematics

Family Buthidae C. L. Koch, 1837

Trypanothacus gen. n.

(Figs. 1–44, 47–77, 84–87, 90–108, 111–118, Tables 1–2)

http://zoobank.org/urn:lsid:zoobank.org:act:E0EABA52-8563-466A-970F-F874A38AEBDC

Buthacus: Hendrixson, 2006: 47–52, figs. 4–5, plates 3–4 (in part); Kovařík et al., 2013: 3 (in part); Kovařík et al., 2016b: 2 (in part); Kovařík, 2018: 6–10 (in part).

Type species. *Trypanothacus barnesi* **sp. n.**

Etymology. The generic epithet *Trypanothacus* (masculine) is formed so as to rhyme with *Buthacus*, presumably a closely allied genus. The latter is deconstructed into Greek terms: βους (bous) = ox, θυσία (thysia) = sacrifice; and Latin ending: *acus* = needle. Here we combine the last two morphemes with Greek τρυπάνι (trypáni) = drill, a reference to the habit of burrowing in more consolidated soils by these scorpions.

Distribution. Saudi Arabia, Oman.

Diagnosis. Medium-sized buthids (Kovařík, 2009; Sissom, 1990), adults 40–60 mm long; carapace trapezoidal with straight anterior margin, without downward-sloped preocular area, surfaces with sparse to moderately dense, fine and coarse granulation interspersed with smooth areas, only anterior median carinae developed, other carinae obsolete, anterior area glossy in females; 5 lateral eyes in 'type 5' pattern (Loria & Prendini, 2014); chelicerae with typical buthid dentition (Vachon, 1963), ventral aspect of fixed finger with two denticles; tergites I–VI with three short, granulose posterior carinae, not projecting beyond posterior margins; tergites I–II with lateral carinae inconspicuous; sternite VII with 2 pairs of weak to moderate carinae; pectines with fulcra, marginal and middle lamellae with dense fine reddish setae; female pectines reach or extend beyond distal end of coxa IV, pectinal tooth counts, ♂ 22–26, ♀ 15–22; hemispermatophore flagelliform, capsule in 3+1-lobe configuration, with 3 sperm hemiduct lobes well separated from flagellum, and small, knob-like basal lobe; sternum subtriangular; metasomal segments moderately robust, segment II as wide as others, segments I–III with 10 carinae, median lateral carinae complete on I, incomplete on II–III; ventromedian carinae on segments II–III well developed with strong denticles that are larger in females, segment V with enlarged lobate dentition on ventrolateral carinae; dorsal carinae of metasoma with sparse medium to long macrosetae in both sexes; telson vesicle bulbous, without subaculear tubercle, aculeus shorter than vesicle; pedipalps short relative to body, femur and patella as long as or shorter than carapace, chelae small with carinae reduced or obsolete, movable finger not more than 1.6 times ventral length of manus, dentate margin of movable finger armed with 7–9 non-imbricated linear subrows of primary denticles or granules, each subrow flanked by internal and external accessory denticles, 3–6 subterminal denticles; males without recess or scalloping of dentate margins at base of pedipalp fingers, chela manus broader than in females; trichobothrial pattern orthobothriotaxic type A (Vachon, 1974); femur with dorsal trichobothria in ß-configuration (Vachon, 1975), petite trichobothrium d_2 located on dorsal surface, e_2 distal to d_5; patella with 7 external, 5 dorsal, and 1 internal trichobothrium, patella d_2 present, d_3 positioned internal to dorsomedian carina; manus with V_1-V_2 axis nearly collinear with long axis of chela, fixed finger with *db* on proximal part of finger between *esb* and *est*, *it* located near tip; legs moderately robust, tibial spurs present on legs III–IV, but spurs may be reduced or absent on leg III; basitarsi I–III compressed, equipped with retrosuperior bristle-comb of macrosetae about as wide as segment, soles of telotarsi with ca. 5–10 unpaired macrosetae near mid-ventral axis, tarsal ungues of moderate to short length, strongly curved and tapered.

Affinities. The ß-configuration of femoral trichobothria, internal position of patella d_3, and 3+1-lobe configuration of hemispermatophore capsule place *Trypanothacus* **gen. n.** firmly in the 'Buthus group', an Old World clade distributed across semi-arid and arid Palaearctic lands (Fet et al, 2005; Kovařík et al., 2016a). Within this group, *Trypanothacus* **gen. n.** is morphologically similar to *Buthacus* Birula, 1908 (under which one of its species was originally described) and *Vachoniolus* Levy et al., 1973. Characters shared by these genera include reduced or obsolete carapacial carination, weakly granular, almost smooth tergites with three short carinae, short pedipalps with reduced carination and fingers bearing linear granule rows with internal and variable external accessory denticles, metasomal segments rather elongate, nearly uniform in width, with variably denticulate ventromedian/ ventrolateral carinae on segments II–III and V, and basitarsal bristle-combs. However, *Buthacus* and *Vachoniolus* are differentiated by the shape of the telson, which has a somewhat pyriform vesicle and a long, curved aculeus

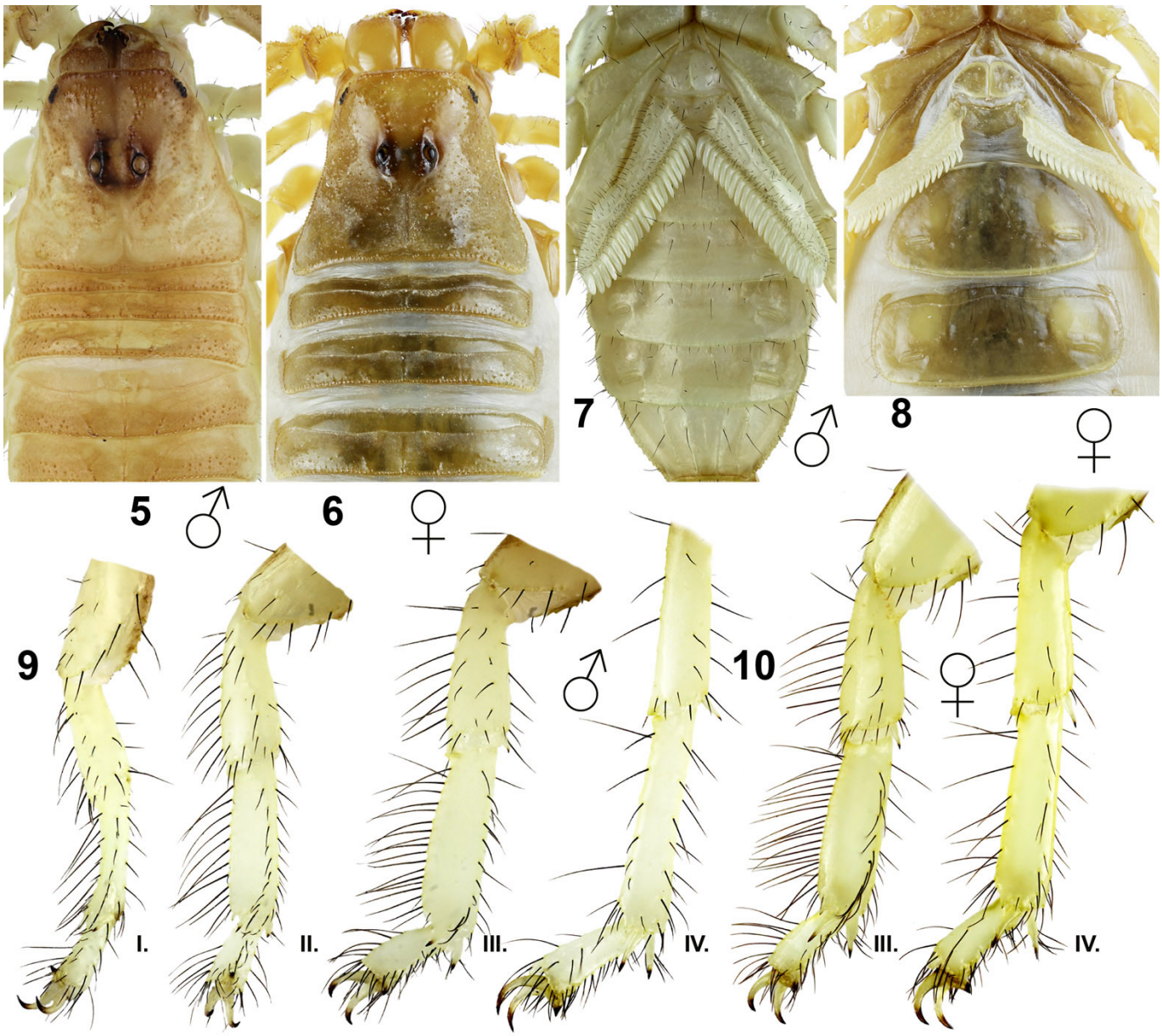

Figures 5–10: *Trypanothacus barnesi* **gen**. et **sp**. **n**. **Figures 5**, **7**, **9**. Male holotype, carapace and tergites I–V (5), coxosternal area and sternites (7), right legs I–IV, retrolateral aspect (9.I–IV). **Figures 6**, **8**, **10**. Female paratype from the type locality, carapace and tergites I–III (6), coxosternal area and sternites III–IV (8), right legs III–IV, retrolateral aspect (10.III–IV).

(aculeus L/ vesicle L 0.74–1.24). This contrasts with the more bulbous vesicle and shorter aculeus of *Trypanothacus* **gen**. **n**. (aculeus L/ vesicle L 0.59–0.76) (Figs. 15–16, 24, 27, 41–42, 45–46, 96, 103, 107). Compared to *Trypanothacus* **gen**. **n**., *Buthacus* and *Vachoniolus* may in some cases also have more slender legs and metasoma, denser setation on dorsal metasomal carinae and soles of telotarsi, and more expansive bristle-combs wider than the basitarsus. *Vachoniolus* is further distingushed by femoral trichobothrium e_2 placed approximately level with or proximal to d_5, and by pronounced sexual dimorphism of pedipalp chelae which are swollen in adult males (Levy et al., 1973; Vachon, 1979; Lowe, 2010b). Apart from these differences, a close relationship of this triad of genera is suggested by the similarity of the hemispermatophore capsules which all have fairly long, lanceolate posterior lobes, and small knob-like basal lobes (Figs. 74–76, 78–81) (see also Levy et al., 1973; Levy & Amitai, 1980; Vachon, 1949, 1952, 1953; Lowe, 2010b). *Trypanothacus* **gen**. **n**. bears some outward resemblance to *Odontobuthus* Vachon, 1950, which also occurs in Oman, and more widely in Iran, Iraq and Pakistan. Both genera have tricarinate tergites, robust legs and metasoma, enlarged dentition on ventromedian carinae of metasoma II–III and ventrolateral carinae of metasoma V, and a bulbous telson with relatively short, stout aculeus. However, *Odontobuthus* is differentiated by: (i) strongly developed carination on the carapace, with distinct central lateral carinae joined to posterior median carinae in a lyre configuration (vs. obsolete carination in *Trypanothacus* **gen**. **n**.); and (ii) hemispermatophore basal lobe a well defined, digitate hook (Lowe, 2010a), that is quite different from the small knob-

like protuberance of *Trypanothacus* **gen**. **n**., *Buthacus* and *Vachoniolus*. Similar parallels and contrasts can be noted when comparing *Trypanothacus* **gen**. **n**. to *Buthus* Leach, 1815, another widespread Old World genus of burrowing buthids.

Subordinate taxa. *Trypanothacus barnesi* **sp**. **n**. and *T. buettikeri* (Hendrixson, 2006) **comb**. **n**..

Comments. We discuss a few other species of *Buthacus* that have been linked to *Buthacus buettikeri* on the basis of diagnostic characters of the metasoma and telson, that may justify transferring them to *Trypanothacus* **gen**. **n**..

(1) Lourenço (2006) incorrectly restored *Buthacus tadmorensis* (Simon, 1892) of Palmyra, Syria, which was synonymized under *Buthacus macrocentrus* (Ehrenberg, 1828) by Kovařík (2005), arguing that the former is distinguished by strongly developed ventromedian carinae on metasoma II–III with enlarged denticles, a character that Simon (1982) cited in his description. However, the Palmyra specimens examined by Lourenço (2006) were characterized only as "... possibly part of the type material of Simon", leaving ambiguity about the identity of this species. The opinion was expressed that *Buthacus leptochelys nitzani* Levy, Amitai & Shulov, 1973, a relatively robust form, could be a junior synonym of *B. tadmorensis*.

Lourenço & Qi (2006) remarked that *B. buettikeri* was similar to, and could be a "regional morph" or synonym of *B. tadmorensis*, because "... the areas of distribution of *B. tadmorensis* and *Buthacus buettikeri* are not very much distinct ...". The latter claim is questionable. Palmyra is far from the localities in central Saudi Arabia where we have confirmed *T. buettikeri* resides based on our restudy of the type series. A few other types from a single, disjunct northern site near the Saudi Arabia-Jordan border, closer to Syria, have not been restudied and their taxonomic status remains unclear (see below). The posterior metasoma and telson of a male from Palmyra labeled as "*B. tadmorensis*" was illustrated in lateral view by Lourenço (2006: 63, fig. 18). If this figure is accurate, the enlarged denticles on ventromedian carinae of metasoma III and ventrolateral carinae of metasoma V are consistent with *T. buettikeri*, but the more slender segments (metasoma IV L/D 2.12, V L/D 2.7), denser setation on dorsal metasomal carinae and ventral telson vesicle, and the less bulbous telson with longer aculeus, are not.

(2) Lourenço & Qi (2006) described *Buthacus pakistanensis* from the Thar Desert of Pakistan. The ventromedian carinae on metasoma II–III and ventrolateral carinae on V are strongly developed, with enlarged teeth in females. The telson is less pyriform, more bulbous, and has a shorter, less strongly curved aculeus compared to other *Buthacus* spp. The authors noted that this species was similar to "*B. tadmorensis*".

(3) Lourenço & Leguin (2009) described *Buthacus williamsi* based on three females collected from the United Arab Emirates in the region of Fujairah; males are unknown. It was suggested to be related to *B. buettikeri*, with which it shares characters of enlarged dentition on ventromedian carinae on metasoma II–III and ventrolateral carinae on V, and a telson with relatively bulbous vesicle and shorter aculeus compared to other *Buthacus* spp. However, it stands apart from both *Buthacus* and *Trypanothacus* **gen**. **n**. in having very short pectines in females, whose apical ends fall well short of the distal limits of coxae IV, and a low pectinal tooth count (13–14) below any recorded from either of those two genera.

Although the aforementioned species bear some similarities to *T. buettikeri* **comb**. **n**., and *T. barnesi* **sp**. **n**., until we can analyze and confirm materials of those species we take a conservative approach and limit the scope of the genus to the two species that we have so far examined. *Trypanothacus* **gen**. **n**. may represent a specialized lineage of the *Buthacus*-complex of psammophiles, that became secondarily adapted to burrowing in firmer substrates. Functional convergence may account for the metasoma and telson structure being similar those of other pelophilous or semi-psammophilous buthids (e.g. *Buthus*, *Odontobuthus*), or of other more robust *Buthacus*-complex species like those discussed above. Future molecular studies (in preparation) should assist in elucidating its phylogenetic position.

Trypanothacus barnesi sp. n.

(Figs. 1–42, 47–77, 84–87, 107–108, 111–118, Tables 1–2)

http://zoobank.org/urn:lsid:zoobank.org:act:B0598EB1-8878-4F09-A850-E36129A16ED0

Type locality and type depository. **Oman**: Dhofar Province, S of Shalim, 18.041070°N 55.612262°E, FKCP.

Type material examined. **Oman**: 1♀ (paratype), Yalooni, Jiddat Al Harasis, 19°57'N 57°06'E, XII.1988, ONHM 1186, Yalooni 185, NHMB; 1♀(paratype), Dhofar, Thamarit, 17°39'N 54°02'E, 10.XI.1989, leg. I. A. J. Brown, ONHM 1416, NHMB; 3♂(paratypes), Thumrait, wadi area SE of Thumrait in slightly raised sedimentary plateau, under sheet wood, and in aircraft shelter, 17°42'N 53°59'E, VII.1997, leg. J. N. Barnes, NHMB, GLPC, ONHM; 1♂ subadult (paratype), Thumrait airfield, in aircraft shelter, 17°42'N, 53°49'E, 23.VII.1998, leg. J. N. Barnes, NHMB; 3♂ (holotype No. 1121 and 2 paratypes No. 1594), S of Shalim, 18.041070°N 55.612262°E, 6.IX.2016, 21:00–23:00 h, full moon, UV detection, FKCP, GLPC (hemispermatophore); 1♀ (paratype), same locality as holotype, 27–28.X.2017, 23:00–01:00 h, 62% moon, UV detection, leg. M. Stockmann, FKCP.

Other material examined. **Oman**: 1juv, near Thamarit, Dhofar, under rock, 450 m a.s.l., 17°40'N 54°02'E, 22.III.1980, leg. J. N. Barnes, Sc74, Barnes 36, MNHN RS8787; 1 ♀ fragment, Yalooni, Jiddat Al Harasis, found dead on level limestone rock and sand, 19°56'N 57°06'E, 10.XI.1980, leg. M. D. Gallagher, MDG6020, NHMB.

Distribution. OMAN. Ranging from the inland plateau of Jiddat al-Harasis in central Oman to the Nejd Desert of Dhofar, southern Oman.

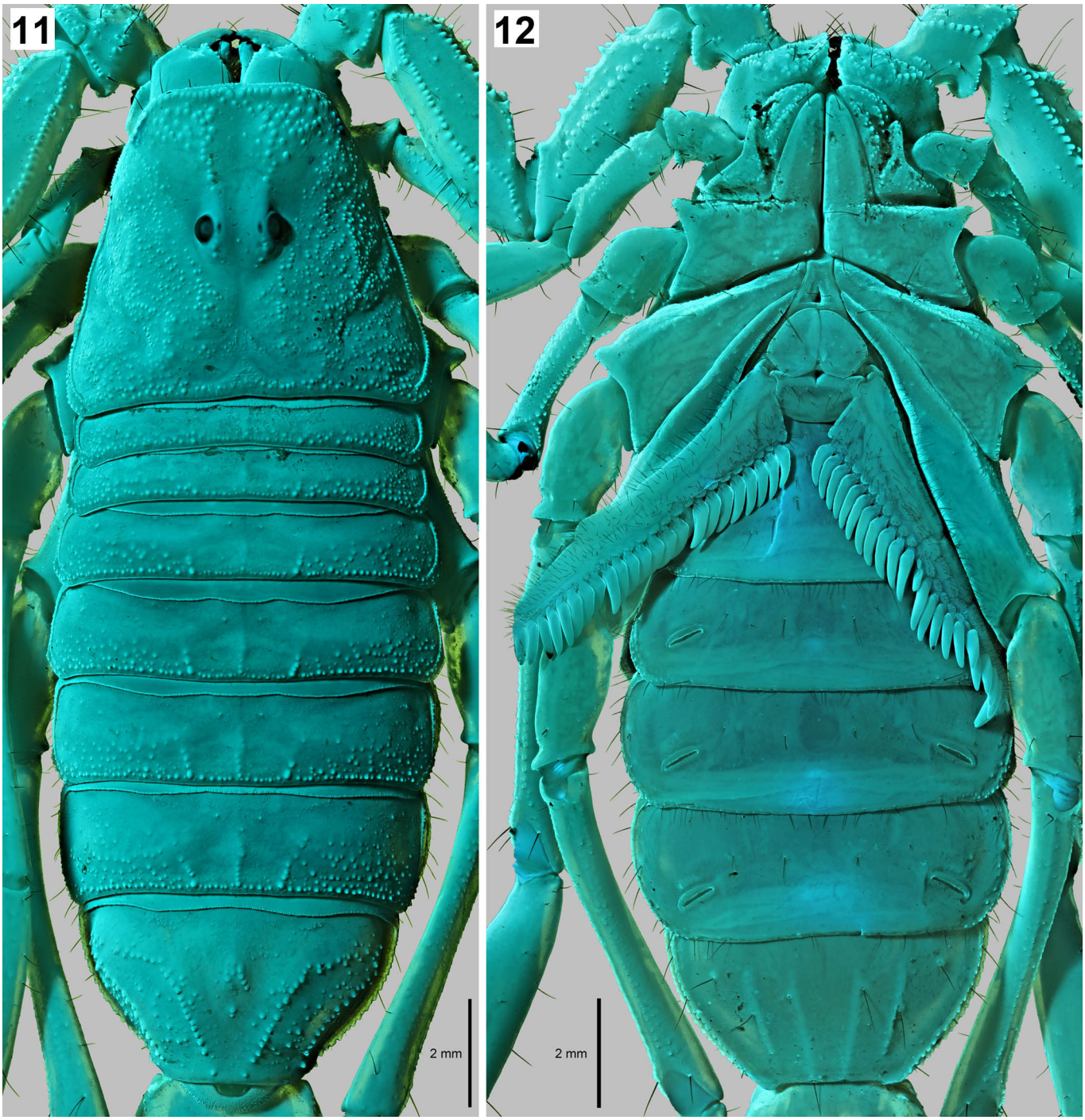

Figures 11–12: *Trypanothacus barnesi* **gen**. et **sp**. **n**. Male paratype from Thumrait (VII.1997), carapace and tergites I–VII (11), coxosternal area and sternites (12). UV fluorescence. Scale bars: 2 mm.

Etymology. The specific epithet is a patronym dedicated to naturalist J. Neil Barnes, Airworks Ltd, Salalah, Oman, who first collected this species in 1980 from around the Thumrait airbase, and contributed other important specimens of Oman scorpions.

Diagnosis. A member of *Trypanothacus* **gen**. **n**. differentiated from its congener as follows: pedipalp femur L/W ♂ 2.6–3.1, ♀ 2.5–2.7, patella L/W ♂ 2.5–2.7, ♀ 2.4–2.7, chela L/W ♂ 3.5–4.0, ♀ 4.4–4.6; metasoma IV L/D ♂ 2.0–2.2, ♀ 1.9–2.0, V L/D ♂ 2.7–3.0, ♀ 2.5–2.9.

Description. Length of adults: ♂ 40–51 mm, ♀ 43–57 mm; habitus as shown in Figs. 1–4.

Coloration (Figs. 1–10, 15–22, 29–42, 71–72, 84–87). Base color yellow or yellowish brown to orange; chelicerae yellow with or without reticulation, dentition reddish to black; median eyes may be surrounded by moderate fuscosity, with weak

		***T. barnesi* gen. et sp. n.**	***T. barnesi* gen. et sp. n.**
Dimensions (MM)		**♂ holotype**	**♀ paratype**
Carapace	L / W	4.849 / 5.733	6.126 / 6.952
Mesosoma	L	9.519	21.43
Tergite VII	L / W	2.843 / 4.934	3.960 / 6.755
Metasoma + telson	L	27.599	29.225
Segment I	L / W / D	3.701 / 3.252 / 2.793	3.758 / 3.702 / 3.197
Segment II	L / W / D	3.947 / 3.058 / 2.850	4.207 / 3.451 / 3.290
Segment III	L / W / D	4.194 / 2.939 / 2.930	4.344 / 3.332 / 3.253
Segment IV	L / W / D	5.120 / 2.791 / 2.530	5.340 / 3.137 / 2.852
Segment V	L / W / D	5.839 / 2.439 / 2.024	6.098 / 2.915 / 2.394
Telson	L / W / D	4.798 / 1.983 / 2.069	5.478 / 2.612 / 2.383
Pedipalp	L	16.036	15.891
Femur	L / W	4.136 / 1.354	4.001 / 1.600
Patella	L / W	4.733 / 1.807	4.743 / 1.948
Chela	L	7.167	7.147
Manus	W / D	1.797 / 1.901	1.600 / 1.836
Movable finger	L	3.929	4.166
Total	**L**	**41.967**	**56.781**

Table 1. Comparative measurements of adults of *Trypanothacus barnesi* **gen**. et **sp**. **n**. Abbreviations: length (L), width (W, in carapace it corresponds to posterior width), depth (D).

fuscosity extending forward towards lateral eyes; articular condyles of pedipalp chela fingers and legs reddish brown; macrosetae of body and appendages dark reddish brown; denticles on pedipalp chela fingers and aculeus of telson dark reddish brown.

Carapace (Figs. 5–6, 11, 13). Trapezoidal, anterior margin straight or almost straight, with weak fine denticulation, 6–12 marginal macrosetae, bordered with row of coarse granules; surface with sparse to moderately dense coarse and fine granulation; anterior median carinae indicated by coarse granules, other carinae of carapace obsolete; lateral areas of interocular triangle with coarse granules, area between anterior median carinae smooth; median ocular tubercle smooth, except for a few posterior granules; median eyes large, well separated; posterolateral areas of interocular triangle, median postocular area and posterior marginal furrow smooth; posterior margin bordered by row of coarse granules; 5 lateral eyes (3 larger, 2 smaller; in 'type 5' configuration of Loria & Prendini, 2014).

Chelicera (Figs. 71–73). Fingers with typical buthid dentition (Vachon, 1963); fixed finger with large distal denticle, one subdistal denticle and two basal denticles fused into bicusp, two denticles on ventral surface, one at level of bicusp, other slightly proximal to subdistal denticle; dorsal margin of movable finger with 5 denticles: one large distal denticle, medium-sized subdistal denticle, large medial denticle, and two small, partially fused basal denticles; ventral margin with 3 denticles: one large distal denticle, and two smaller denticles in medial and basal positions.

Mesosoma (Figs. 1–4, 6, 8, 11–14). *Tergites* I–VI tricarinate with median carina and anteriorly diverging pair of lateral carinae; carinae coarsely granular, the lateral pair on the tergites I–II possibly indistinct; all carinae short with only ca. 2–5 granules, confined to posterior half or third of tergite; lateral flanks of tergites with sparse to moderately dense, coarse granulation on posterior half, posterior margins bordered with row of granules; other tergite surfaces smooth to faintly shagreened; tergite VII pentacarinate, median carina a granulated hump, lateral carinae well developed, coarsely granular; posterior margin of tergite VII without rim of granules, intercarinal surfaces smooth or with sparse, coarse granulation; coxae mostly smooth, with few sparse isolated patches of granules, coxal margins smooth or with weak granulation; sternum subtriangular, smooth, with deep posteromedian pit; *sternites* with smooth surfaces and posterior margins, III–VI without carinae, VII with 2 pairs of weak to moderate, smooth to granulated carinae; *sternal chaetotaxy*: sternite III-VI posterior margins conspicuously setose, bearing approximately 20 macrosetae, III bearing about a dozen macrosetae on medial surface, IV-VII with 4 medial and 2 lateral macrosetae, VII with single anterior macroseta on each of the 4 carinae, plus a lateral pair; *pectines* with anterior margins extending to midpoint (♂) or to approximately proximal 1/6 (♀) of trochanter IV, with 3 marginal lamellae, 4–9 middle lamellae; lamellae and fulcra bear numerous short, fine, dark macrosetae; pectine basal piece and genital opercula smooth with fine macrosetae; pectinal tooth counts, ♂ 22–26, ♀ 17–21.

Hemispermatophore (Figs. 74–77). Flagelliform, moderately elongated, trunk ca. 6 times length of capsule region as

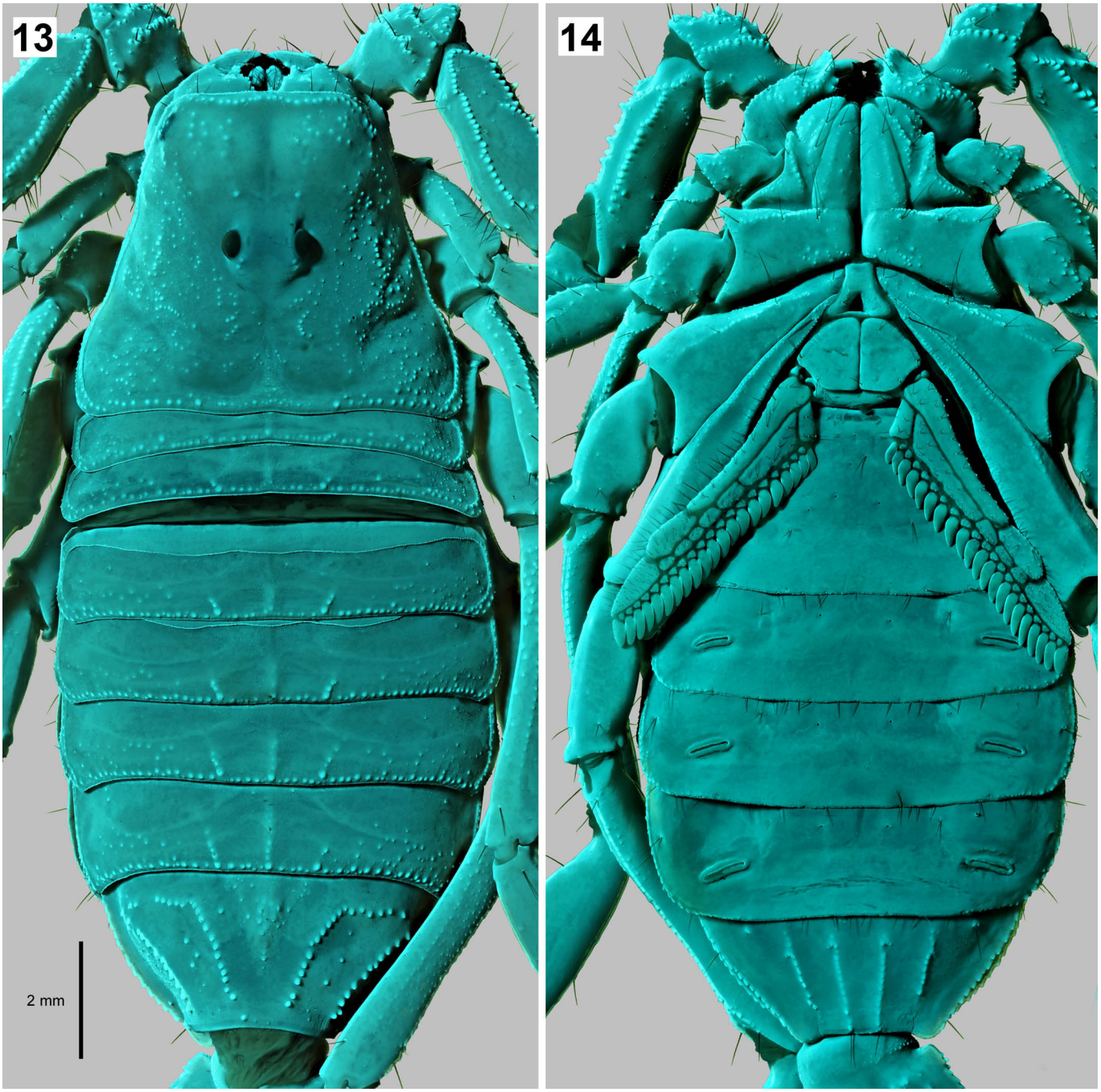

Figures 13–14: *Trypanothacus barnesi* **gen**. et **sp**. **n**. Female paratype from Yalooni (XII.1988), carapace and tergites I–VII (13), coxosternal area and sternites (14). UV fluorescence. Scale bar: 2 mm.

measured from proximal flagellum base; flagellum well separated from capsule lobes, pars recta short, ca. 2.7 times length of capsule and lobes, 50% length of trunk, with weak fin along anterior margin; pars reflecta long, narrow, gradually tapered, hyaline, 0.88 times length of trunk; capsule region with 4 lobes arranged in '3 +1' configuration, posterior lobe the largest, a lanceolate lamina with pointed apex; median lobe smallest, acuminate, attached to base of posterior lobe along short, suture, but a sclerotized carina not clearly visible; anterior lobe of intermediate length, laminate, apically acuminate; basal lobe a small, rounded knob-like process situated well proximal from point of splitting of posterior and median lobes.

Metasoma and telson (Figs. 15–28). *Metasoma* I with 10 granulated or crenulated carinae, median lateral carinae complete, ventromedian carinae may be weak or obsolete in males; II–III with 10 granulated or crenulated carinae, median lateral carinae incomplete, indicated by ca. 5–14 granules on posterior 1/3 to 2/3 of segment; ventromedian and ventrolateral carinae on II–III stronger in females, with conspicuously enlarged, dentate or lobate granules, increasing in size posteriorly; coarsely granulose anterior ventral margins present on III–IV; IV with 8 granulated or crenulated carinae; V with 5 carinae, dorsolateral carinae weak, granulated, ventrolateral carinae strong, irregularly crenulated with several enlarged,

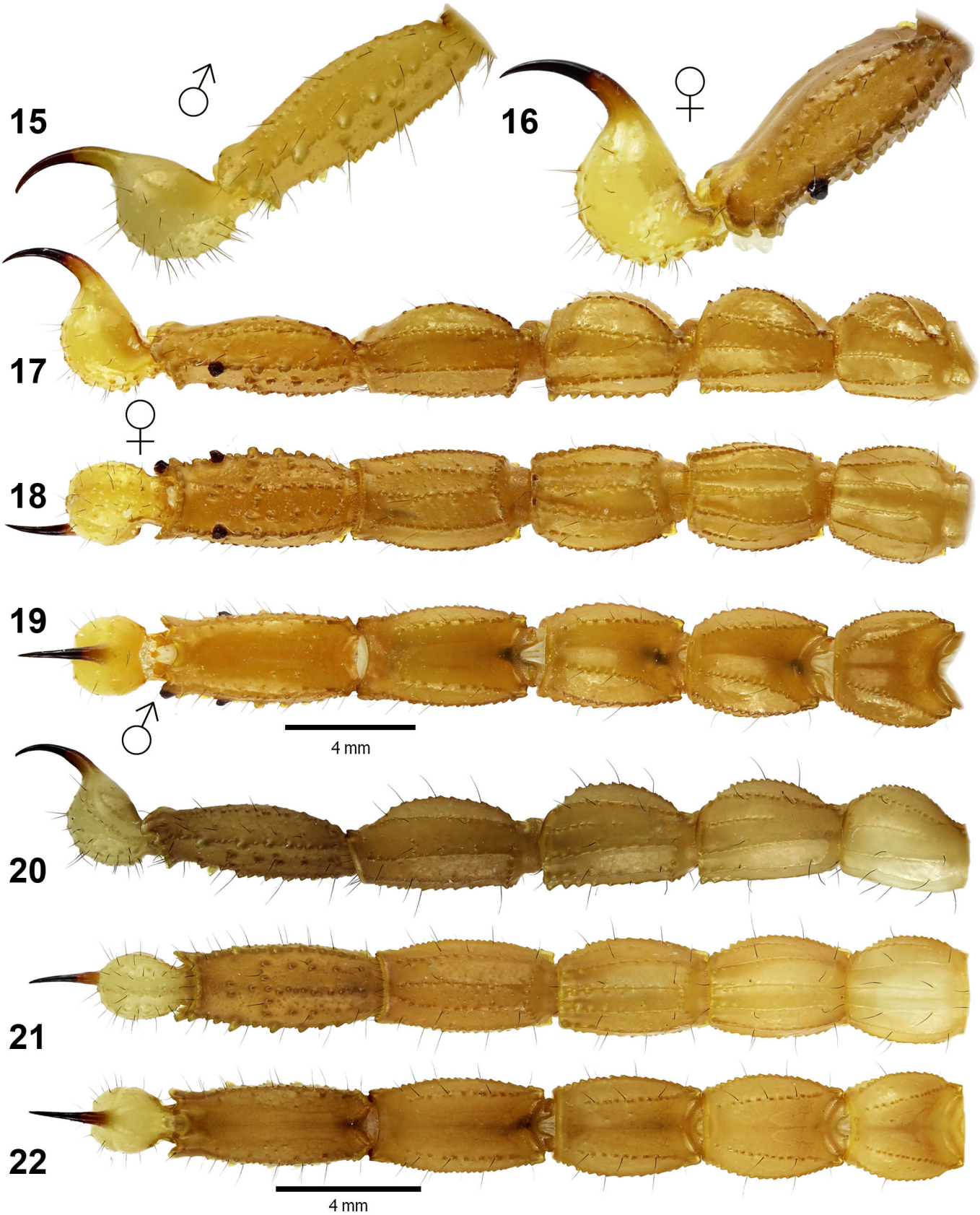

Figures 15–22: *Trypanothacus barnesi* **gen**. et **sp**. **n**. **Figures 15**, **20–22**. Male holotype, metasoma V and telson lateral view (15), metasoma and telson lateral (20), ventral (21), and dorsal (22) views. **Figures**. **16–19**. Female paratype from type locality, metasoma V and telson lateral view (16), metasoma and telson lateral (17), ventral (18), and dorsal (19) views. Scale bars: 4 mm (17–19, 20–21).

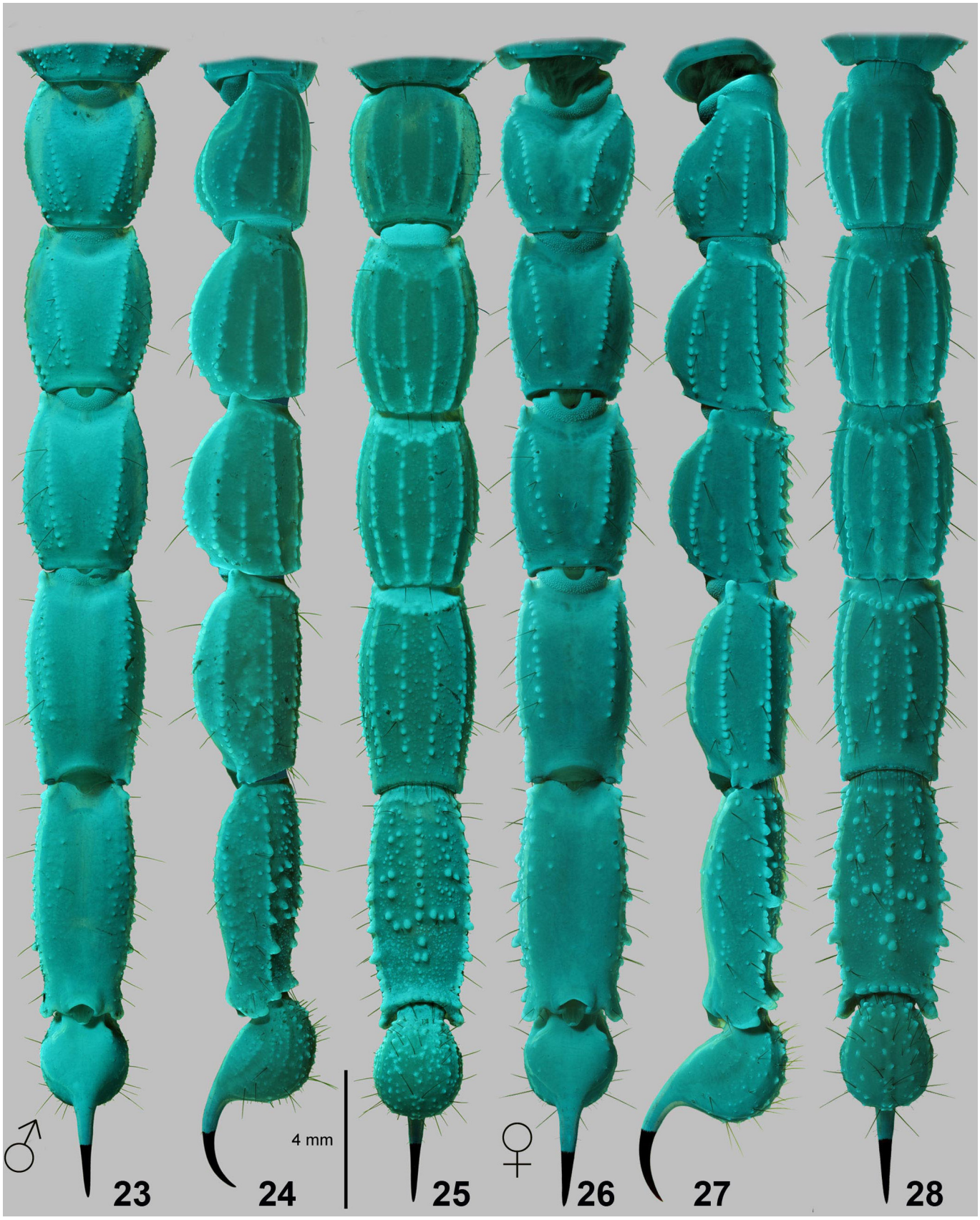

Figures 23–**28**: *Trypanothacus barnesi* **gen**. et **sp**. **n**. **Figures 23**–**25**. Male paratype from Thumrait (VII.1997), metasoma and telson dorsal (23), lateral (24) and ventral (25) views. **Figures 26**–**28**. Female paratype from Yalooni (XII.1988), metasoma and telson dorsal (26), lateral (27) and ventral (28) views. UV fluorescence. Scale bar: 4 mm.

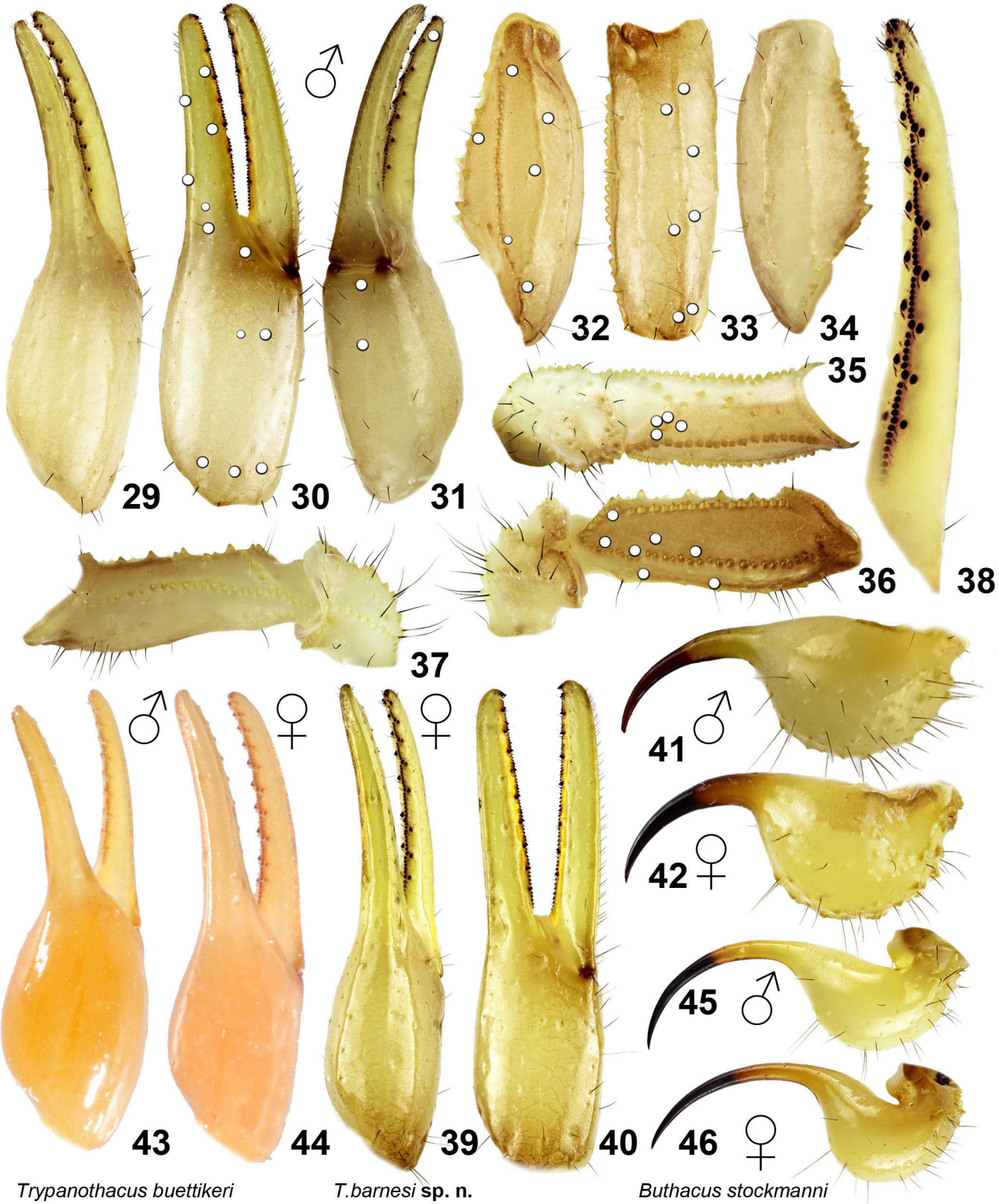

Figures 29–46: **Figures 29–42**: *Trypanothacus barnesi* **gen**. et **sp**. **n**. **Figures 29–40**. Pedipalp segments. **Figures 29–38**. Male holotype, chela dorsal (29), external (30), and ventral (31) views. Patella dorsal (32), external (33) and ventral (34) views. Femur and trochanter internal (35), dorsal (36), and ventral (37) views. Movable finger dentition (38). Trichobothrial pattern is indicated in Figures 30–33 and 35–36. **Figures 39–40**. Female paratype from the type locality, chela dorsal (39) and external (40) views. **Figures 41–42**. Telson, male holotype (41) and female paratype from type locality (42), lateral views. **Figures 43–44**: *T. buettikeri* **comb**. **n**., pedipalp chela dorsal, male holotype (43) and female paratype (44). **Figures 45–46**: *Buthacus stockmanni* Kovařík et al., 2016, telson, male holotype (45) and female paratype (46), lateral views.

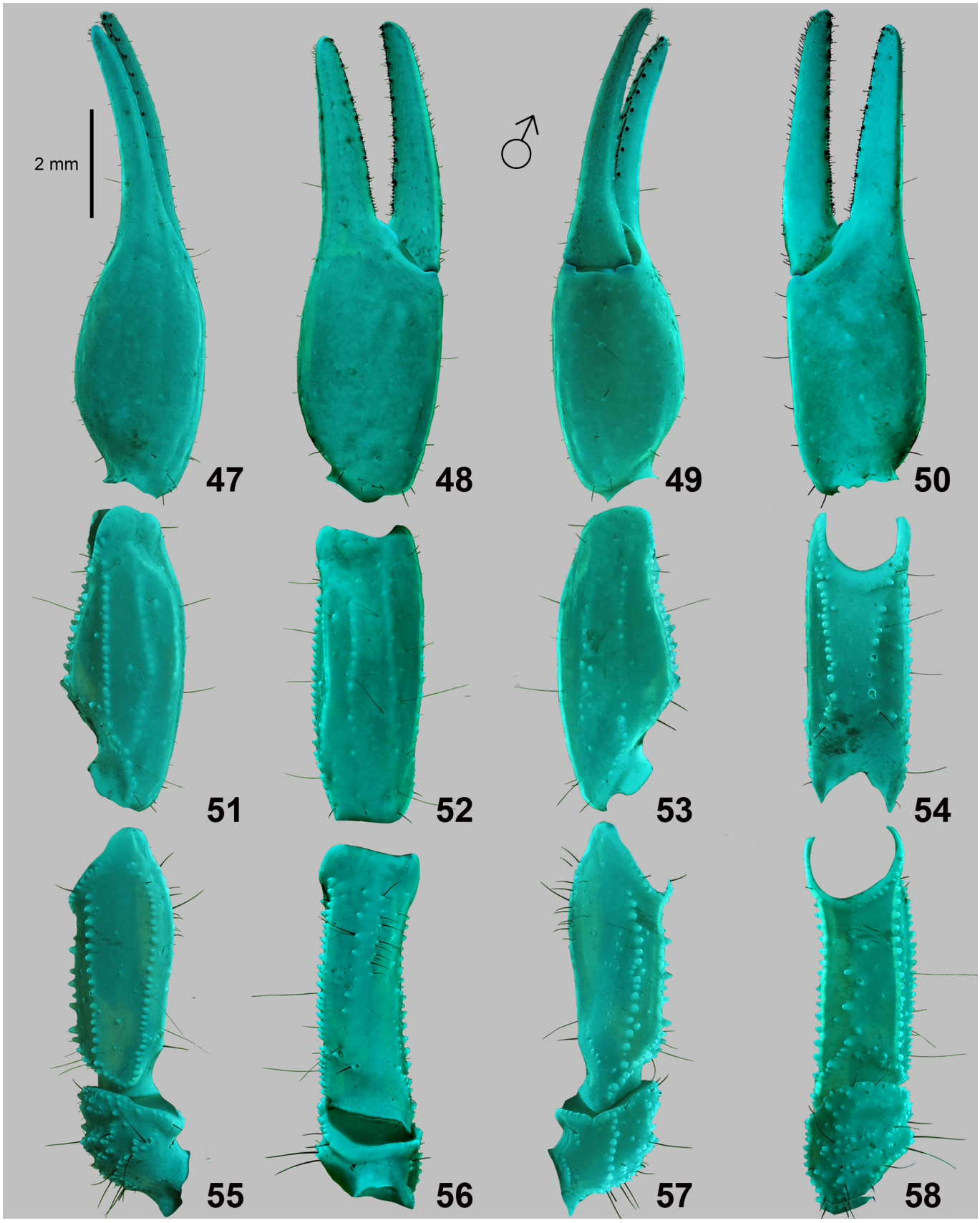

Figures 47–58: *Trypanothacus barnesi* **gen**. et **sp**. **n**. Pedipalp segments of male paratype from Thumrait (VII.1997), chela dorsal (47), external (48), ventral (49) and internal (50) views. Patella dorsal (51), external (52), ventral (53) and internal (54) views. Femur and trochanter dorsal (55), external (56), ventral (57) and internal (58) views. UV fluorescence. Scale bar: 2 mm.

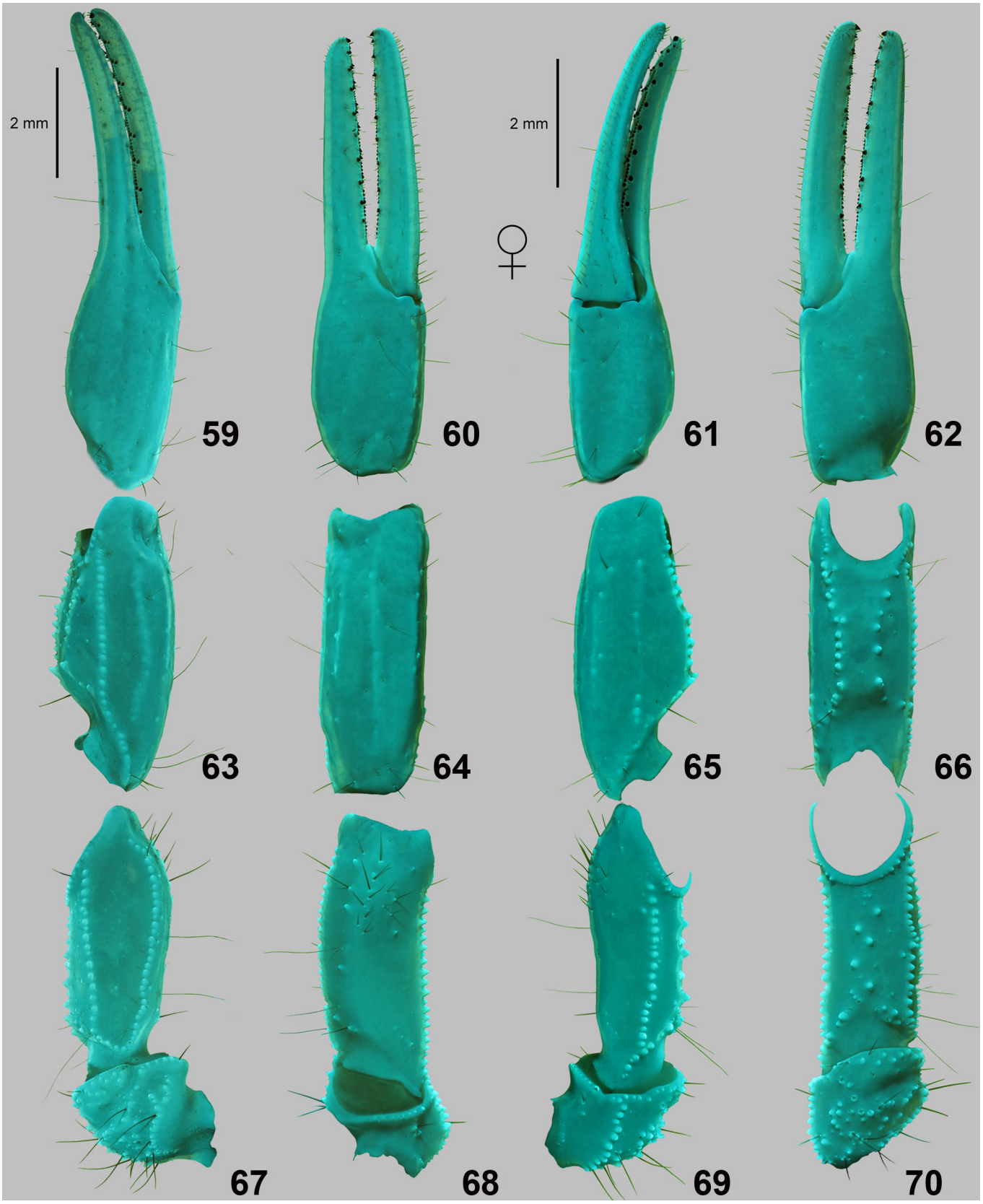

Figures 59–70: *Trypanothacus barnesi* **gen**. et **sp**. **n**. Pedipalp segments of female paratypes, chela dorsal (59), external (60), ventral (61) and internal (62) views. Patella dorsal (63), external (64), ventral (65) and internal (66) views. Femur and trochanter dorsal (67), external (68), ventral (69) and internal (70) views. Dorsal views (59, 63, 67): paratype female from Thumrait (XI.1989) (with normal dorsointernal carina on femur). External (60, 64, 68), ventral (61, 65, 69) and internal (62, 66, 70) views: paratype female from Yalooni (XII.1988) (with malformed dorsointernal carina on femur). UV fluorescence. Scale bars: 2 mm (59, 63, 67), 2 mm (60–62, 64–66, 69–70).

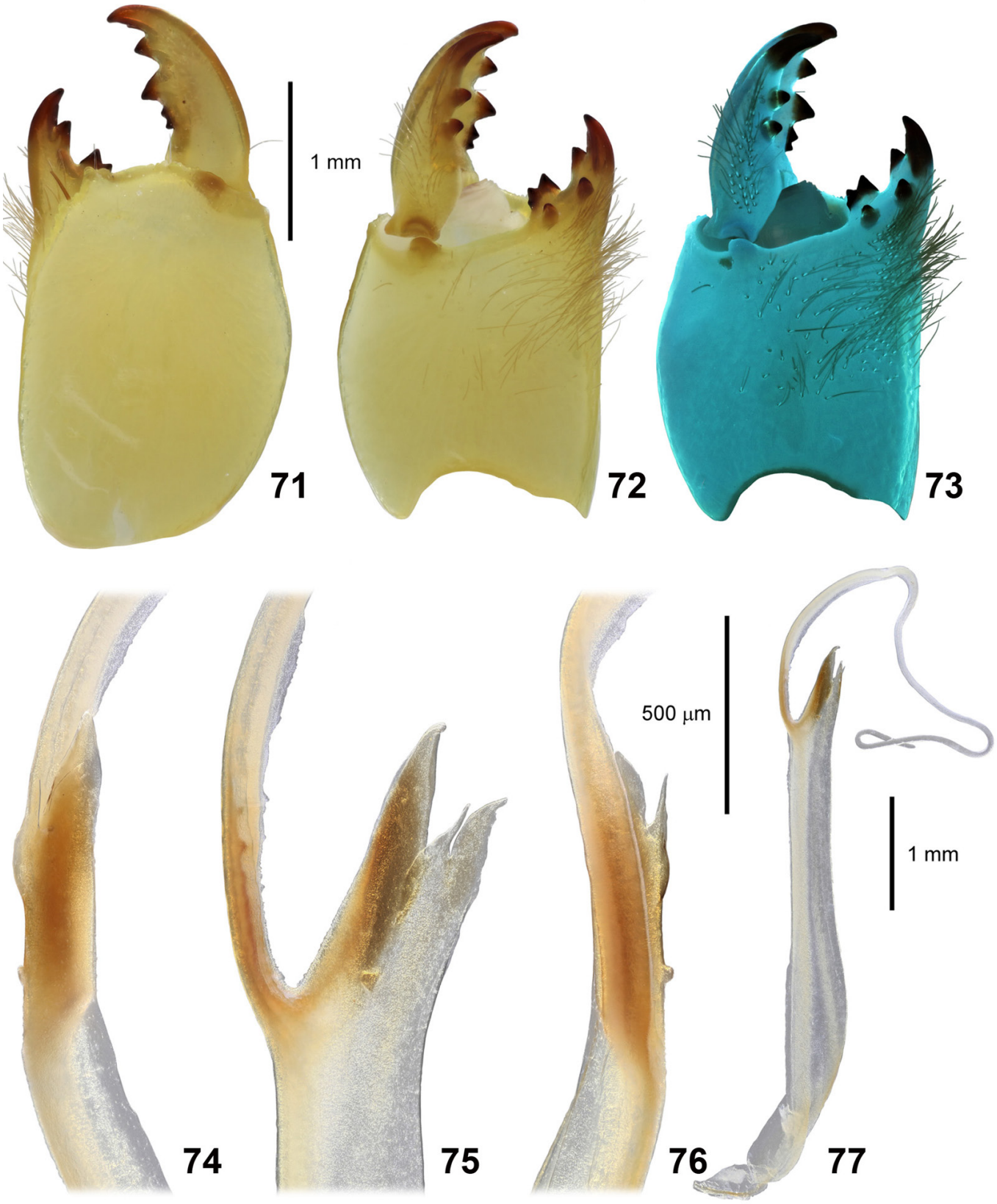

Figures 71–77: *Trypanothacus barnesi* **gen**. et **sp**. **n**. **Figures 71–73**. Paratype male, right chelicera, dorsal (71), ventral (72) and ventral UV fluorescence (73) views. Scale bar: 1 mm. **Figures 74–77**. Holotype male, right hemispermatophore, capsule region with lobes in anterior (74), convex compressed (75) and posterior (76) views, and whole hemispermatophore in convex view (77). Scale bars: 1 mm (71–73), 500 µm (74–76), 1 mm (77).

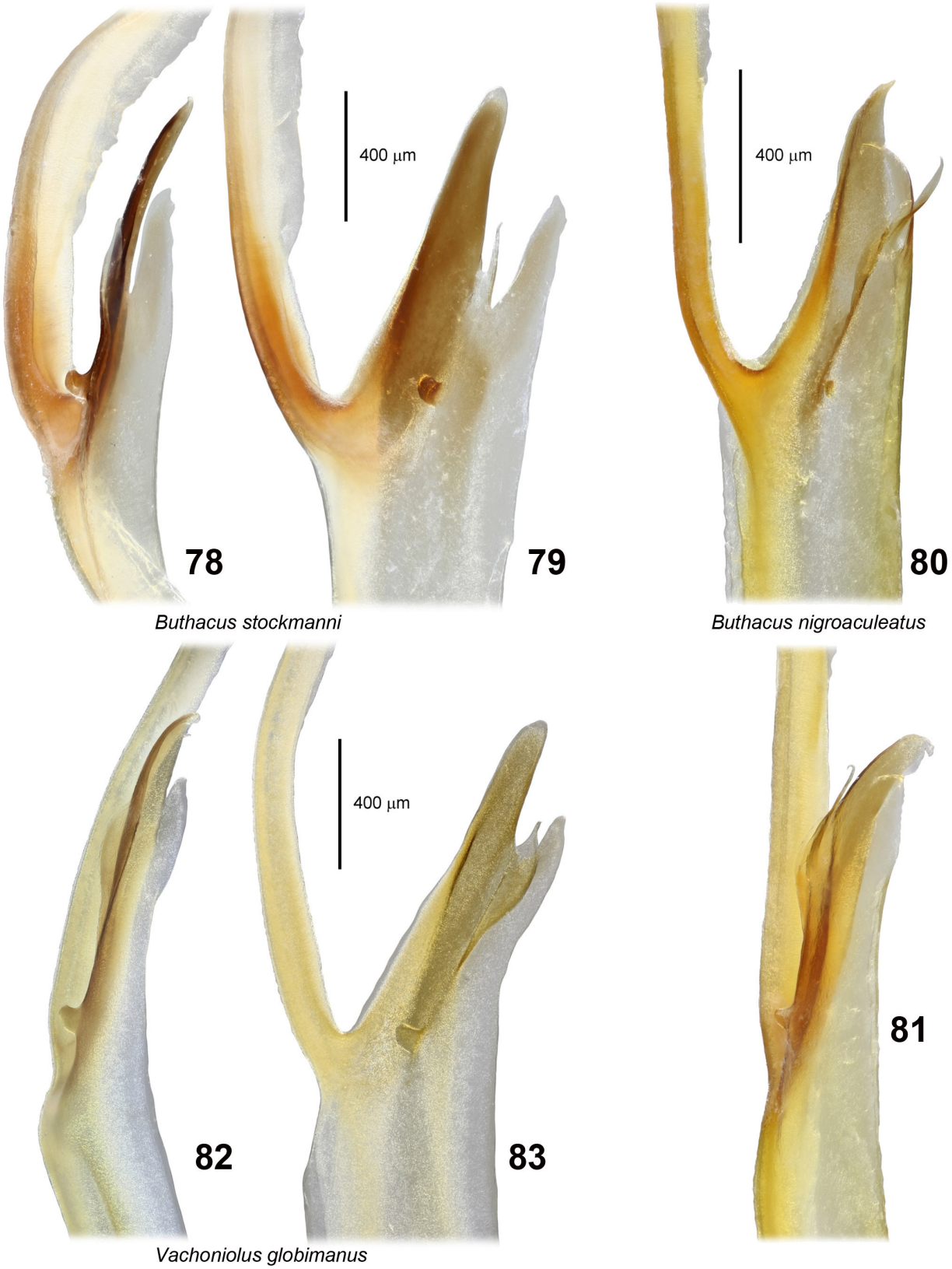

Figures 78–83: Hemispermatophore capsule regions and lobes of buthid genera presumed to be closely related to *Trypanothacus* **gen. n.**. **Figures 78–79**: *Buthacus stockmanni* Kovařík, Lowe et Šťáhlavský, 2016 (topoparatype male, N. of Zag, Morocco). **Figures 80–81**: *Buthacus nigroaculeatus* Levy, Amitai et Shulov, 1973 (Wadi Muqshin, Montesar, Oman, 30.III.1989, leg. A.S. Gardner). **Figures 82–83**: *Vachoniolus globimanus* Levy, Amitai et Shulov, 1973 (Ramlat As Sahmah, Oman, 7.X.1994, leg. G. Lowe & M.D. Gallagher). All figures right capsule except Figures 78–79 (mirrored left). Anterior (78, 81–82) and convex compressed (79–80, 83) views. Scale bars: 400 µm (78–79), 400 µm (80–81), 400 µm (82–83).

Figures 84–85: *Trypanothacus barnesi* **gen**. et **sp**. **n**., in vivo habitus, male holotype (84) and female paratype from type locality (85).

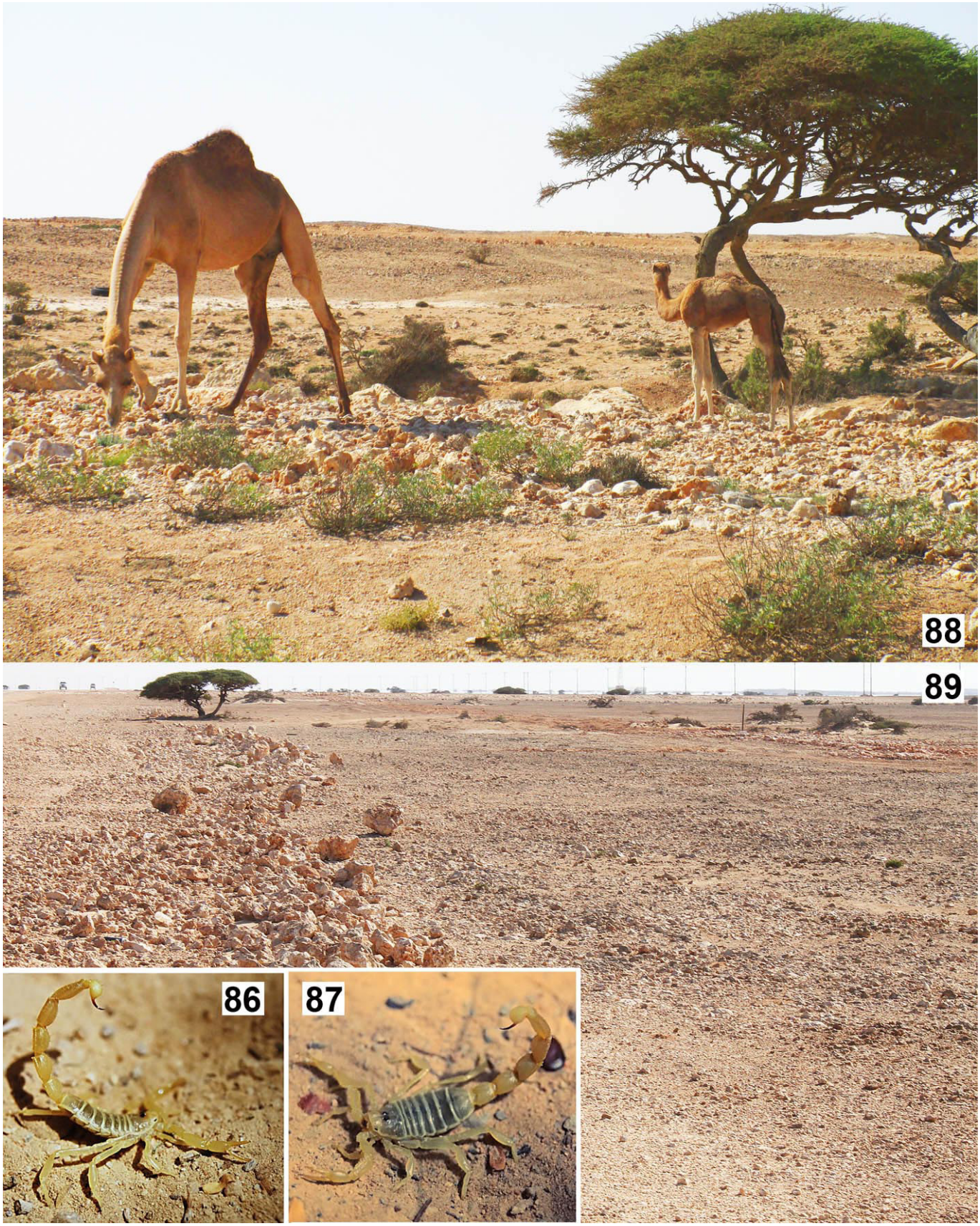

Figures 86–89: *Trypanothacus barnesi* **gen**. et **sp**. **n**.. **Figures 86–87**. Male (86) and female (87) from Thumrait, photos by J. N. Barnes. **Figures 88–89**. Type locality, Oman, S of Schelim, 18.041070°N 55.612262°E.

RATIO	range ♂	mean ± sd (N) ♂	range ♀	mean ± sd (N) ♀
carapace W/L	1.098 – 1.182	1.137 ± 0.037 (4)	1.135 – 1.252	1.211 ± 0.052 (4)
pedipalp femur L/ carapace L	0.811 – 0.876	0.841 ± 0.029 (4)	0.653 – 0.739	0.706 ± 0.039 (4)
pedipalp femur L/W	2.609 – 3.055	2.805 ± 0.185 (4)	2.501 – 2.647	2.574 ± 0.080 (4)
pedipalp patella L/W	2.543 – 2.653	2.603 ± 0.046 (4)	2.435 – 2.723	2.539 ± 0.130 (4)
pedipalp chela L/W	3.557 – 3.988	3.739 ± 0.212 (4)	4.467 – 4.589	4.525 ± 0.052 (4)
pedipalp movable finger L/ manus ventral L	0.958 – 1.249	1.109 ± 0.122 (4)	1.502 – 2.025	1.645 ± 0.254 (4)
pedipalp fixed finger L/ manus ventral L	0.853 – 1.023	0.908 ± 0.077 (4)	1.200 – 1.251	1.228 ± 0.023 (4)
pedipalp manus W/D	0.888 – 0.947	0.919 ± 0.027 (4)	0.842 – 0.900	0.866 ± 0.026 (4)
pedipalp manus ventral L/ manus W	1.714 – 1.879	1.779 ± 0.071 (4)	1.287 – 1.889	1.696 ± 0.276 (4)
metasoma I L/W	1.111 – 1.138	1.120 ± 0.013 (4)	0.985 – 1.086	1.032 ± 0.043 (4)
metasoma II L/W	1.291 – 1.418	1.356 ± 0.052 (4)	1.203 – 1.299	1.255 ± 0.051 (4)
metasoma III L/W	1.405 – 1.526	1.455 ± 0.053 (4)	1.304 – 1.387	1.357 ± 0.039 (4)
metasoma IV L/W	1.753 – 1.887	1.818 ± 0.057 (4)	1.702 – 1.785	1.751 ± 0.036 (4)
metasoma V L/W	2.256 – 2.500	2.389 ± 0.101 (4)	2.092 – 2.286	2.178 ± 0.099 (3)
metasoma I L/D	1.284 – 1.352	1.316 ± 0.029 (4)	1.147 – 1.315	1.210 ± 0.074 (4)
metasoma II L/D	1.385 – 1.569	1.512 ± 0.086 (4)	1.279 – 1.414	1.359 ± 0.067 (4)
metasoma III L/D	1.431 – 1.610	1.556 ± 0.083 (4)	1.335 – 1.528	1.473 ± 0.092 (4)
metasoma IV L/D	1.997 – 2.191	2.100 ± 0.104 (4)	1.872 – 2.031	1.955 ± 0.073 (4)
metasoma V L/D	2.763 – 2.955	2.846 ± 0.091 (4)	2.547 – 2.855	2.737 ± 0.166 (3)
metasoma II W/ metasoma I W	0.940 – 0.977	0.954 ± 0.017 (4)	0.932 – 0.973	0.944 ± 0.019 (4)
metasoma IV W/ metasoma I W	0.858 – 0.912	0.874 ± 0.026 (4)	0.847 – 0.884	0.865 ± 0.015 (4)
metasoma V W/ metasoma I W	0.711 – 0.788	0.741 ± 0.036 (4)	0.760 – 0.809	0.785 ± 0.024 (3)
leg III patella L/W	3.017 – 3.336	3.133 ± 0.176 (3)	2.721 – 2.903	2.788 ± 0.100 (3)
pectine anterior margin L/ carapace L	0.940 – 1.242	1.101 ± 0.128 (4)	0.633 – 0.994	0.816 ± 0.181 (3)

Table 2. Variation in morphometric ratios of adult *Trypanothacus barnesi* **gen**. et **sp**. **n**. Abbreviations: length (L), width (W, in carapace it corresponds to posterior width), depth (D), standard deviation (sd).

lobate granules that become larger posteriorly; ventromedian carina of V composed of series of large granules interspersed with finer granulation; intercarinal surfaces of I–IV smooth or almost smooth dorsally, almost smooth or with sparse granules dorsolaterally and laterally; ventrolateral and ventral surfaces of I smooth, of II–III almost smooth with sparse fine granulation, of IV with weak, fine granulation or shagreened; segment V smooth dorsally with scattered small granules, with weak fine granulation laterally, slightly denser fine granulation ventrally; lateral anal arch divided into 2–3 lobes; ventral anal arch armed with regular series of ca. 5–7 coarse granules; *telson* with distinctly bulbous vesicle bearing coarse granules on ventral surface; granulation more dense in males, more sparse in females, with smooth areas; lateral surface of vesicle with sparser granulation, dorsal surface smooth; aculeus equal to or shorter than vesicle in length, moderately curved; subaculear tubercle absent; *chaetotaxy*: metasomal segments and telson sparsely setose; long macrosetae located along carinae on metasoma I–IV, typically 2–3 per carina; V with several setae along dorsolateral carina, ca. 6 setae in longitudinal series on lower lateral surface, several setae on ventral surface associated with enlarged granules; telson vesicle with a dozen or more long macrosetae scattered over ventral and ventrolateral surfaces.

Pedipalps (Figs. 29–40, 47–70). Segments short, robust; *femur* with 3 strong, granulated carinae: dorsoexternal, dorsointernal, and ventrointernal, other carinae obsolete; dorsal, lateral and ventral surfaces smooth except for few small solitary granules, internal surface smooth except for several solitary coarse granules; distal external surface with group of ca. dozen macrosetae; *patella* with 7 carinae: dorsointernal, internal and ventrointernal carinae coarsely granulose, internal carina with sparse, non-contiguous granules; dorsomedian and dorsoexternal carinae weak, smooth or almost smooth with traces of coarse granules; external and ventroexternal carinae weak, smooth; ventromedian carina obsolete, indicated by series of few granules; all intercarinal surfaces smooth; setation very sparse, with few large solitary macrosetae on carinae; *chela* smooth, carinae obsolete with residual traces of carinae in females; few large macrosetae present, ventral surface of movable finger with numerous short macrosetae, increasing in density distally; dentate margin of movable and fixed fingers with 7–8 rows of granules, each with a single external and internal accessory granule, and 3–6 subterminal granules (typically 3–4 of them enlarged); trichobothrial pattern orthobothriotaxic type Aβ, chela fixed finger with *db* near base of fixed finger.

Legs (Figs. 1–4, 9–10). Legs with long femora and robust patellae, tibiae and tarsi; femora with few solitary macrosetae; tibiae I–III with dorsal (retrosuperior) linear series of long macrosetae (= tibial 'bristle comb', 8–12 setae in sample of N=13 leg III segments), and shorter macrosetae on other surfaces; basitarsi I–III compressed, with two linear series of shorter ventral (proinferior and retroinferior) macrosetae, single linear series of longer dorsal (retrosuperior) macrosetae (= basitarsal 'bristle comb', 17–23 setae in sample of N=12 leg III segments); macrosetae long and thin in both sexes; leg IV without basitarsal compression, longer than legs I–III, long macrosetae more sparse, not arranged in linear series; leg I–IV femora and patella with indications of 4–6 carinae, which are usually obsolete; paired ventral carinae on femora granulate or denticulate, prolateral surfaces of femora with weak granulation localized on inferior proximal areas of I–II; tibial spur on leg IV strong, longer than spur on leg III; prolateral pedal spurs basally bifurcate, setose (leg III spur with 6–8 short macrosetae in sample of N=10 segments); retrolateral pedal spurs simple.

Sexual dimorphism. Compared to females, males have longer pectines (Figs. 2, 4, 7–8, 12, 14), higher pectinal tooth counts, and broader pedipalp chelae; chela fingers are straight in both sexes, and males lack recess or scalloping of the proximal dentate margins (Figs. 29–31, 39–40, 47–50, 59–62, Table 1); the male telson vesicle is slightly less bulbous, granulation on the carapace and tergites is more dense; sternite VII carinae of the male are weaker and smoother, and metasomal carinae are not as robust as in females, especially the ventromedian carinae on metasoma II–III; intercarinal granulation is more dense on the male metasoma. For data on morphometric sexual dimorphism, see under species diagnosis and Table 2.

Measurements. See Table 1.

Morphometric variation. See Table 2.

Karyotypes (Figs. 111–113). We analyzed two males (holotype and paratype from type locality) using standard cytogenetic methods (e. g. Kovařík et al., 2009). The diploid number of both specimens is 26 chromosomes (Figs. 111–112). We did not observe chiasmata during male meiosis and centromeres on chromosomes. These characteristics are typical for the scorpions from the family Buthidae (e.g. Mattos et al., 2013). The chromosomes of *Trypanothacus barnesi* **sp**. **n**. gradually decrease in length from 8.69 % to 5.92 % of the halpoid set (Fig. 113).

Affinities. In the diagnosis, we separated *T. barnesi* **sp**. **n**. from its similar allopatric congener, *T. buettikeri* **comb**. **n**. by measurable differences in the shapes of the pedipalp and metasoma, indicated by non-overlapping ranges of morphometric ratios. *T. barnesi* **sp**. **n**. is a less robust, more slender scorpion with narrower pedipalps and posterior metasomal segments. Only limited numbers of specimens of *T. buettikeri* **comb**. **n**. were available to us for study and confirmation of species identity, and additional material may extend morphometric variation in this species. However, samples from around the type locality and a well separated western site (Wadi Turabah) both have robust segments, so the morphometric diagnosis is likely to remain valid. We hypothesize that *T. barnesi* **sp**. **n**. and *T. buettikeri* **comb**. **n**. are sister species that diverged after southern and northern populations were isolated from each other by formation of the Rub' al Khali (Empty Quarter) dune system during the Quaternary. Soft unstabilized sands may be an effective physical barrier blocking dispersal of ancestral *Trypanothacus* adapted to firmer substrates. This model of vicariant speciation by dune barriers has also been suggested for *Leiurus macroctenus*, a sympatric scorpion that may have substrate preferences similar to those of *T. barnesi* **sp**. **n**. (Lowe et al., 2014).

Comments on localities and life strategy. The type locality is a flat desert plateau along route 42, the road between Shalim and Ash Shuwaymiyyah near the coast. The substrate consists of reddish soil alternating with bare rock, clay and sand. Shrubs and trees are scattered and provide only slight patches of humidity in an otherwise arid area. There are few if any loose rocks, except in disturbed areas where stones may be piled near the road by construction activity. The weather on both collection dates was mild at night (ca. 22 °C) with high humidity, barely any wind and no clouds to block the bright moon. At night, *Trypanothacus barnesi* **sp**. **n**. was the most active scorpion in this area. Males were highly active on open ground, whilst females were resting in ambush position at the entrances of their burrows. The burrows were located in sandy areas at the bases of shrubs or rocks, and only rarely on open ground. Only small juveniles to medium-sized immatures were found under rocks without a burrow. Far more males than females were observed on both nights. Remarkably, many were observed actively foraging and feeding on termites, close to the insect nests and trails. Several termites were captured and consumed simultaneously by one scorpion. Other potential prey, including various insects (Formicidae, Heteroptera, Coleoptera, Blattodea, lepismatids) and arachnids (ticks, spiders and pseudoscorpions) were abundant in the area. Mobile white mites were observed on many individuals of *T. barnesi* **sp**. **n**. (cf. Fig. 85, an adult female with mites on tergite II and carapace), but not on other arthropods in this habitat. Some individual scorpions were densely covered with mites, whereas others bore only a few. Other species of scorpions found in this area were: *Androctonus crassicauda* (Olivier, 1807), *Leiurus macroctenus* Lowe, Yağmur & Kovařík, 2014, *Femtobuthus shutuae* Lowe, 2010, *Nebo* sp., and *Compsobuthus acutecarinatus* (Simon, 1882).

Both the type locality and the paratype collection site of Yalooni (Arabian Oryx sanctuary) are located on the Jiddat Al Harasis, an extensive stony limestone plateau in central Oman. The region is ecologically classified as coastal fog desert. Moisture is deposited by condensation of humid air swept inland from the sea during the summer monsoon (khareef). This sustains local vegetation and animal populations, including the scorpion fauna. The other collection sites around Thumrait are located on the Nejd Desert plain in the rain shadow of the Jabal Qara mountains. Without monsoon mist, the terrain is more arid, consisting mostly of sand and

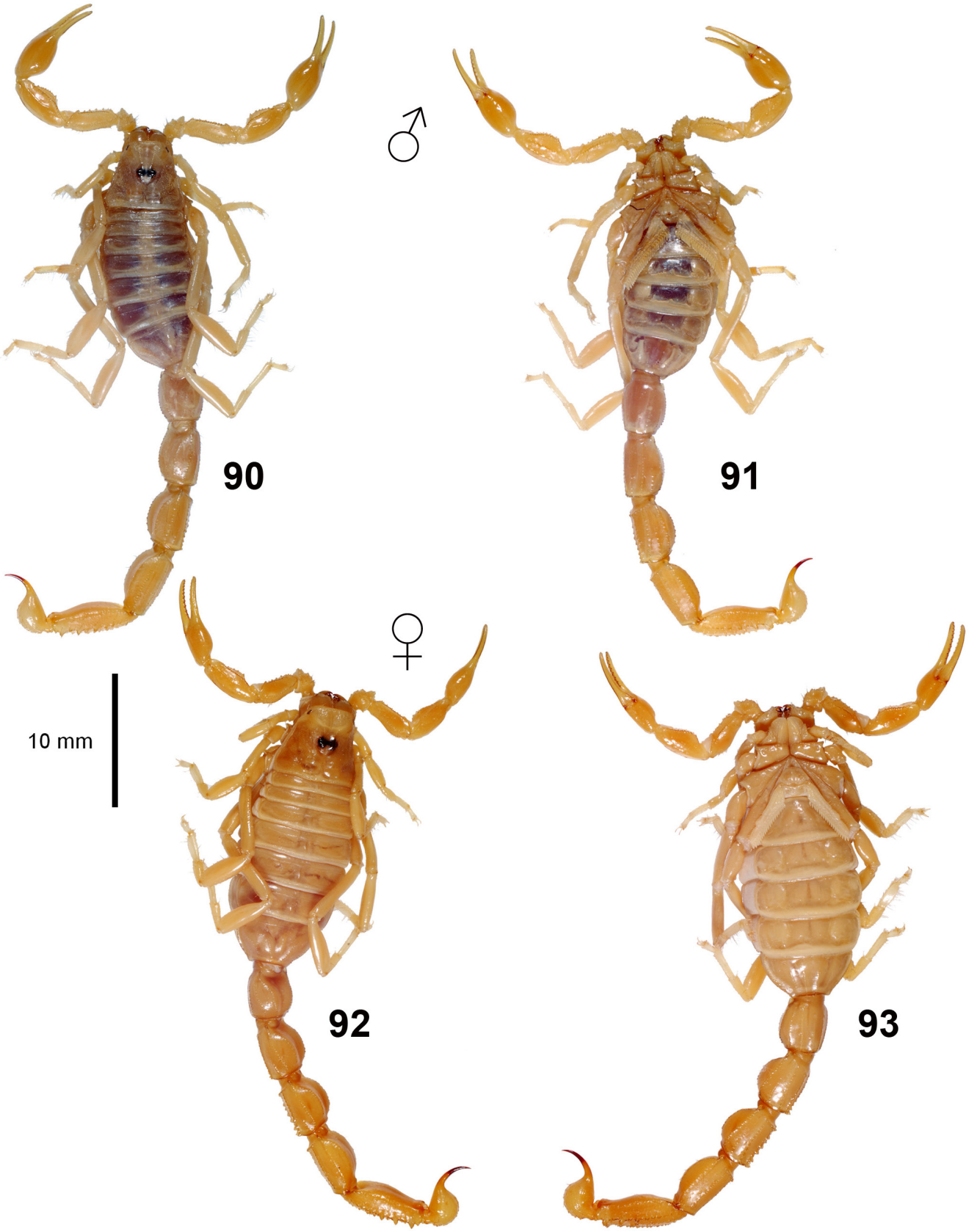

Figures 90–93: *Trypanothacus buettikeri* **comb. n**. **Figures 90–91**. Male holotype in dorsal (90) and ventral (91) views. **Figures 92–93**: Female paratype in dorsal (92) and ventral (93) views. Scale bars: 10 mm .

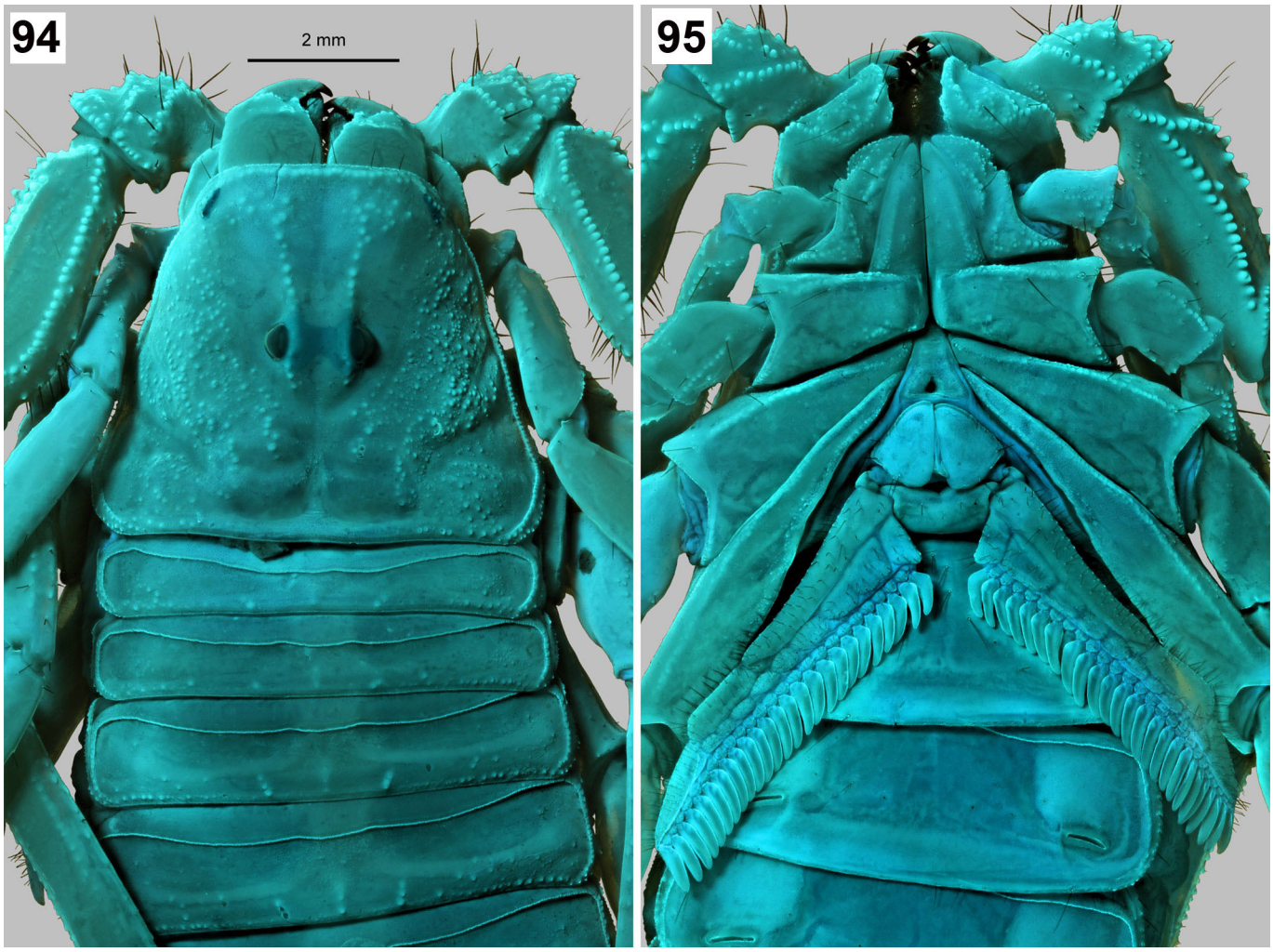

Figures 94–95: *Trypanothacus buettikeri* **comb**. **n**. Male holotype, carapace and tergites I–IV (94), coxosternal area and sternites I–II (95). UV fluorescence. Scale bar: 2 mm.

gravel flats with sporadic rocky outcrops. Drainage in some shallow wadi beds supports scattered trees and shrubs, with xerophytic herbs and grass as low ground cover. In this area, *T. barnesi* **sp**. **n**. was reported to be present but uncommon (J.N. Barnes, personal communication, 05.VII.1992, Figs. 86–87). Other scorpions recorded from there were: *Androctonus crassicauda*, *Leiurus macroctenus*, *Orthochirus innesi* Simon, 1910 and *Xenobuthus anthracinus* (Pocock, 1895). The first two of these were the most common.

Captive rearing and breeding. Two medium-sized immatures (1♂, 1♀) were reared to maturity in captivity. They were housed in 11 cm × 11cm × 6 cm plastic boxes with two perforated sides, filled with a thin layer of loose sand, and were provided with a small shelter. A burrowing substrate was not provided in order to more easily observe behavior. Average temperatures in summer were 32°C (day) and 24°C (night). In winter, a mild diapause was simulated with temperatures of about 25°C (day) and 20°C (night). One corner of the box was slightly moistened by spraying water once a week to provide drinking water. The water completely evaporated in the following day and conditions were kept dry for the rest of the week to prevent mycosis. Insects (*Thermobia domestica*, *Shelfordella lateralis* and *Acheta domesticus*) of adequate sizes were offered as prey.

Three weeks after attaining maturity, the female was mated (XI. 2017). Upon being introduced to the female, a male immediately initiated courtship without preliminary behavior like juddering. The promenade à deux began with the male grasping the female pedipalps, and continued with a series of back and forth pulling motions by both sexes (Fig. 114). Male pectinal movements occurred almost continually, without lengthy interruptions. Remarkably, both sexes engaged in sand scraping with legs I–III (Fig. 115), sometimes settling their bodies into depressions they excavated in the loose sand to rest for a few seconds (Fig. 116) before continuing the promenade à deux. Several episodes of cheliceral massage lasting several seconds were observed (Fig. 117), but there was no sexual sting. After 17 min 48 s, a spermatophore was deposited by the male on a flat rock (Fig. 118) and taken up by the female 3 s later. Both individuals then immediately separated, and the female began to display aggressive behavior towards the male, but did not attempt mate cannibalism. The female was subsequently reared under the same conditions as described

above, and gave birth to 23 juveniles in the following season (VII. 2018). These were separated from the parent one week after their first ecdysis, and successfully reared under the same conditions as the parental generation.

Trypanothacus buettikeri (Hendrixson, 2006), **comb**. **n**.
(Figs. 90–108)

Buthacus buettikeri Hendrixson, 2006: 47–52, figs. 4–5, plates 3–4 (in part); Lourenço & Qi, 2006: 161; El-Hennawy, 2009: 121, 126; Lourenço & Leguin, 2009: 104, 107, tab. 1; Desouky & Alshammari, 2011: 195–196, figs. 6–7 (?) (in part); Kovařík et al., 2013: 3; El-Hennawy, 2014: 45; Kovařík et al., 2016b: 2; Kovařík, 2018: 7.

Type locality and type depository. **Saudi Arabia**, Um ad-Dabah, NHMB.

Type material examined. **Saudi Arabia**: 1♂ (holotype), Um ad-Dabah [23°54'N 45°01'E, 920 m a.s.l.], 13.V.1980, leg. W. Büttiker, NHMB 0587 (=172a); 1♀ (paratype), Khashm Dhibi [23°50'N 45°05'E, 750 m a.s.l.], 10.X.1981, leg. W. Büttiker, NHMB 0896 (=172e); 3♀1 juv. (paratypes), Kushm Dibi [24°14'N 46°05'E, 850 m a.s.l.], 30.I.1981, leg. W. Büttiker, NHMB 172cd.
other material examined.1♂ (fragmented), Wadi Turabah [25°30'N 41°17'E, 1,430 m a.s.l.], XII.1986, leg. W. Büttiker, NHMB Sc509.

Distribution. SAUDI ARABIA. Central plateau, Najd desert; east of Harrat Khaybar lava field, east of Hijaz mountains.

Diagnosis. A member of *Trypanothacus* **gen**. **n**. differentiated from its congener as follows: pedipalp femur L/W ♂ 2.5, ♀ 2.2; pedipalp patella L/W ♂ 2.1–2.2, ♀ 2.3, chela L/W ♂ 3.2–3.6, ♀ 4.0; metasoma IV L/D ♂ 1.8–2.0, ♀ 1.9, V L/D ♂ 2.4–2.6, ♀ 2.4.

Comments. Hendrixson originally described *Buthacus buettikeri* on the basis of a series of specimens from several localities in Saudi Arabia (Hendrixon, 2006: 47, 51). We examined part of the type series and concluded that the holotype male (No. 172a; Figs. 43, 90–91, 94–101) and paratype females from Khashm Dhibi (Nos. 172cd, NHMB 0896=172e; Figs. 44, 92–93, 103–106), from the Najd plateau region of central Saudi Arabia, belong to *Trypanothacus* **gen**. **n**.. However, several other specimens of the type series from widely disjunct sites along the western slopes of the Asir ranges (facing the Red Sea Coast), differed from the holotype and are associated with the *Buthacus leptochelys* (Ehrenberg, 1829) species complex of the genus *Buthacus* (i.e., female paratypes including NHMB 515=172b, 630=172f and 620=172g; from Jabal al-Ghamdiyah, Wadi Maraum, Addar, Kijat (examined); also likely including MNHN RS8425 from Makkah By-pass, based on specimen photographs on the MNHN website). In light of these misidentifications, the status of other MNHN paratypes from a widely disjunct site near the northern border of Saudi Arabia (ca. 1,030 km from the type locality) remains unclear.

Desouky & Alshammari (2011) recorded *B. buettikeri* from the Ha'il region in the central plateau of Saudi Arabia (Hufair, Sarraa near Al-Ghazala), on "sandy desert". In photographs, their adult female (carapace L 5.92 mm) (fig. 7) appears morphometrically consistent (e.g. patella L/W 2.57, metasoma I L/W 1.02) with females of the type series that we have examined, however their adult male (carapace L 6.4 mm) (fig. 6) has markedly different morphometrics with much more slender pedipalps and metasoma (e.g. pedipalp patella L/W 2.95, metasoma I L/W 1.38) than in the male types of *B. buettikeri*. It is also more slender than all males of *T. barnesi* **sp**. **n**. in our type series. This would seem to indicate large variation in male morphometrics of *B. buettikeri*, maybe reflecting local geographic races as Ha'il is located some distance northwest of the type locality. However, a large adult male that we determined as *T. buettikeri*, has morphometrics more robust than the holotype, yet was collected from Wadi Turabah, relatively closer to the Ha'il region. As we have not studied Ha'il region material, we withhold judgement on the taxonomic status of those populations, but the large morphometric difference likely indicates a different species. Desouky & Alshammari (2011: 196) assumed *B. williamsi* Lourenço & Leguin, 2009, to be a junior synonym of *B. buettikeri*, but did not justify this by comparative study of the types of either species. They also claimed that the telson and aculeus in *B. buettikeri* was "clearly more slender and elongated" than in *B. leptochelys*, misrepresenting Hendrixson (2006), when the opposite is true.

Affinities. See comments under *T. barnesi* **sp**. **n**.

Discussion

The genus *Trypanothacus* **gen**. **n**. is separated from *Buthacus* primarily by the form of the telson, with a strongly bulbous vesicle and a relatively short aculeus that is distinctly shorter than the vesicle. In *Buthacus*, the vesicle is less bulbous, moderately pyriform or tear drop-shaped, and the aculeus is longer, and in many species longer than the vesicle (Figs. 41–42 versus Figs. 45–46). Although the aculeus in *Buthacus* spp. may appear more curved than in *Trypanothacus* **gen**. **n**., this is a visual illusion created by its greater length. In fact, the *Trypanothacus* **gen**. **n**. aculeus is more strongly curved, bending more tightly to achieve a terminal tip angle similar to that of *Buthacus* in a shorter distance. Tip angles relative to horizontal were (mean ± sem): *Buthacus* 94.39° ± 2.18° (N = 26; 21 species, 17♂, 9♀), *Trypanothacus* **gen**. **n**. 94.39° ± 2.18° (N = 4; 2 species, 2♂, 2♀), p = 0.53, two-tailed t-test, i.e. not significantly different. Radii of curvature normalized to vesicle length were (in the same samples): *Buthacus* 0.59 ± 0.01, *Trypanothacus* **gen**. **n**. 0.41 ± 0.02, $p = 8.4 \times 10^{-7}$, one-tailed t-test, i.e. on average, *Trypanothacus* **gen**. **n**. had a significantly tighter curvature.

To visualize variation and differences in telson shape across taxa, we plotted vesicle length/ depth (L/D), a measure of elongation (smaller values indicate more bulbous), against

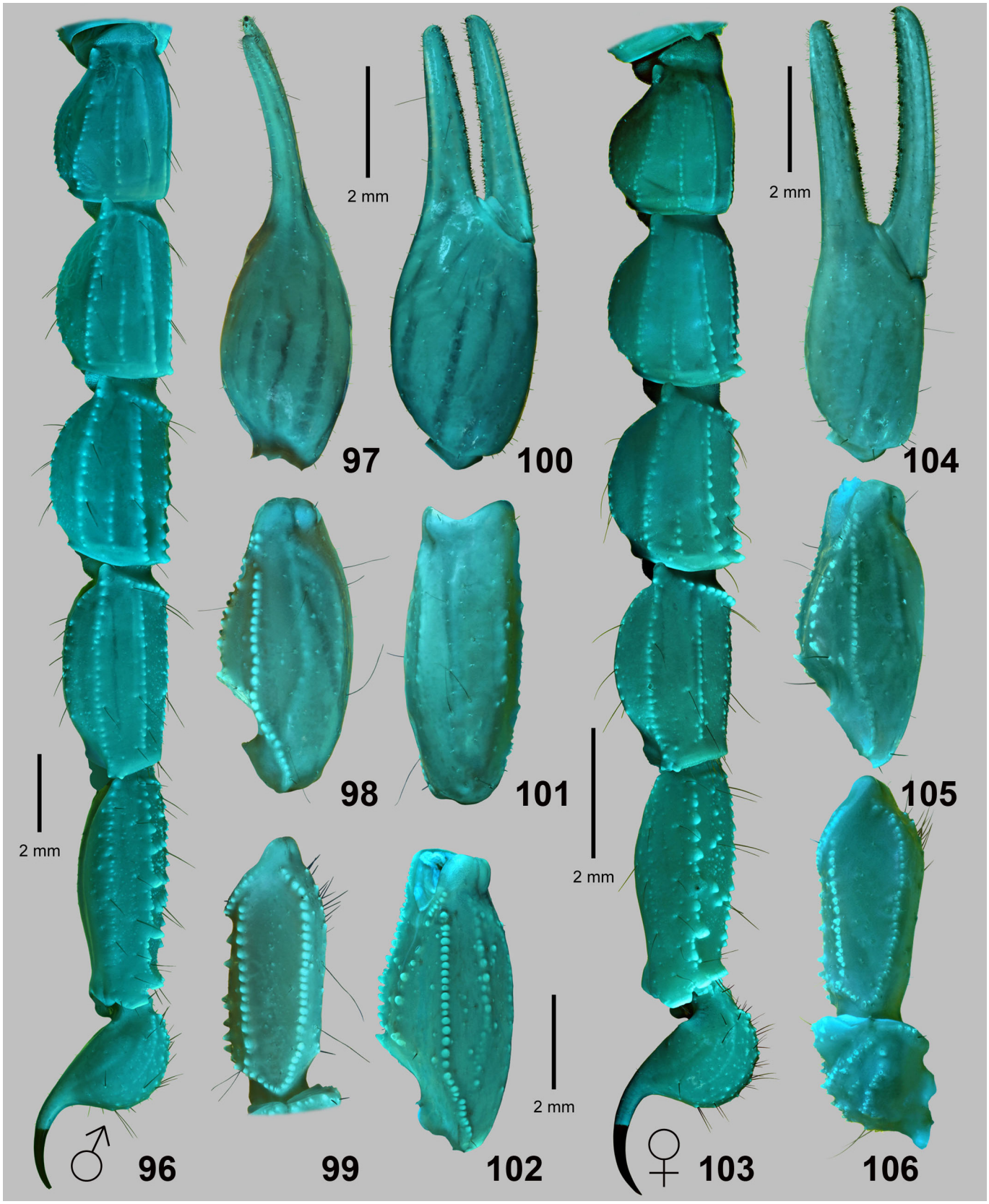

Figures 96–106: *Trypanothacus buettikeri* **comb**. **n**. **Figures 96–101**. Male holotype, lateral view of metasoma and telson (96), dorsal views of pedipalp chela (97) patella (98) and femur (99), external views of pedipalp chela (100) and patella (101). **Figure 102**. Male from Wadi Turabah (NHMB No. 509), dorsal view of pedipalp patella. **Figures 103–106**. Female paratype (NHMB 896), lateral views of metasoma (103) and pedipalp chela (104), dorsal view of pedipalp patella (105) and femur (106). UV fluorescence. Scale bars: 2 mm (96), 2 mm (97–101), 2 mm (102), 2 mm (103), 2 mm (104–106).

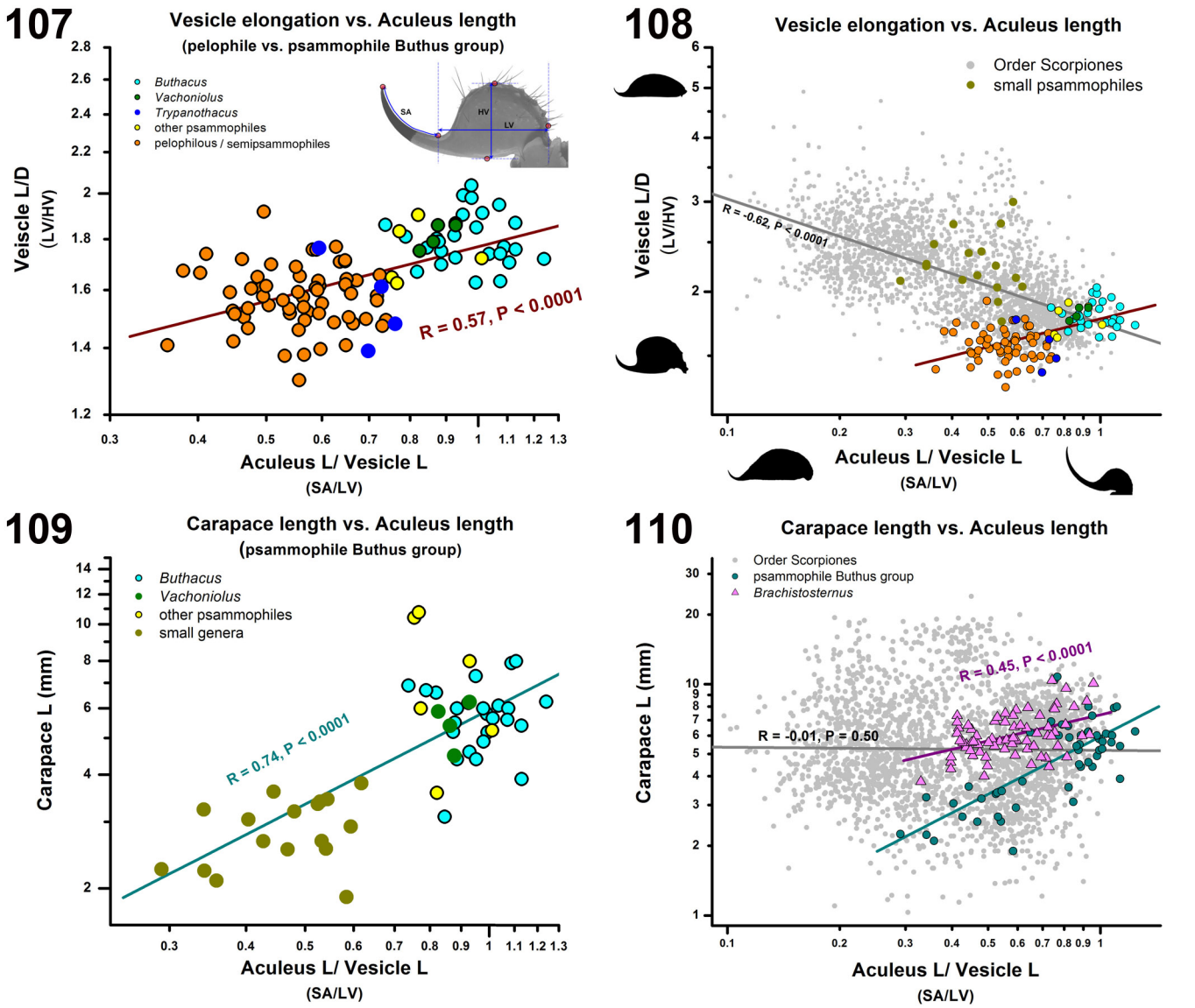

Figures 107–110: Morphometric scaling relations of the telson of fossorial 'Buthus group' scorpions. **Figure 107**. Double logarithmic scatterplot of telson vesicle length/ depth (L/ D) ratio vs. aculeus length normalized to vesicle length (aculeus L/ vesicle L), for large pelophiles/ semi-psammophiles (4 genera, 53 species) (*Buthus*, *Odontobuthus*, *Pantobuthus*: orange circles; *Trypanothacus* **gen. n.**: blue circles) and large psammophiles/ ultrapsammophiles (6 genera, 29 species) (*Buthacus*: cyan circles; *Vachoniolus*: dark green circles; *Apistobuthus*, *Buthiscus*, *Liobuthus*, and *Plesiobuthus*: yellow circles). Dark line: linear least squares regression fit to all data shown (Pearson correlation coefficient, R = 0.57). Upper right inset: diagram of measurements estimated from inverted telson lateral profiles, with dorsal surface of vesicle approximately leveled; SA = ventral profile length of aculeus from base point to tip, LV = length of vesicle from anterior limit or inflection point to aculeus base point; HV = vesicle depth or height (distance between dorsal and ventral tangent planes). Base point was placed at local minimum of inverted ventral profile curve. SA was calculated by cubic spline fit (>10 anchor points). For a minority of broken tips, SA was estimated by intersecting extrapolated dorsal and ventral profile curves (< 5%). **Figure 108**. Scatterplot of fossorial buthids in Figure 107, superposed upon larger scale plot of Order Scorpiones (gray circles). Gray line: linear least squares regression fit to Order Scorpiones data (including data in Figure 107) (Pearson correlation coefficient, R = –0.62). Also plotted are data from small 'Buthus group' psammophiles/ ultrapsammophiles (5 genera, 10 species: *Compsobuthus arabicus*, *Lanzatus somalilandus*, *Neobuthus kutcheri*, *Picobuthus dundoni*, *P. wahibaensis*, *Anomalobuthus krivochatskyi*, *A. pavlovskyi*, *A. rickmersi*, *A. lowei*, *A. talebii*) (dark yellow circles). **Figure 109**. Double logarithmic scatterplot of carapace length (L) vs. aculeus length normalized to vesicle length (i.e., aculeus L/ vesicle L) for psammophile/ ultrapsammophile members of the 'Buthus group', including large species in Figure 107, and small species in Figure 108 (dark yellow circles). Blue line: linear least squares regression fit to all data shown (Pearson correlation coefficient, R = 0.74). **Figure 110**. Scatterplot of psammophile buthid data in Figure 109 (all in one color, blue circles) superposed upon larger scale plot of Order Scorpiones (gray circles). Gray line: linear least squares regression to Order Scorpiones data (including data in Figure 109) (Pearson correlation coefficient, R = –0.01). Also plotted are data from bothriurid genus *Brachistosternus* (43 species) (magenta triangles), and corresponding linear least squares regression fit (R = 0.39). All plots in Figures 107-110 include data from both males and females. Data were assembled by mining taxonomic literature or directly measuring specimens. Included are 1854 species or subspecies (1331 ♂, 1201 ♀) representing all known extant genera (1841 species or subspecies) plus 7 fossil genera (13 species).

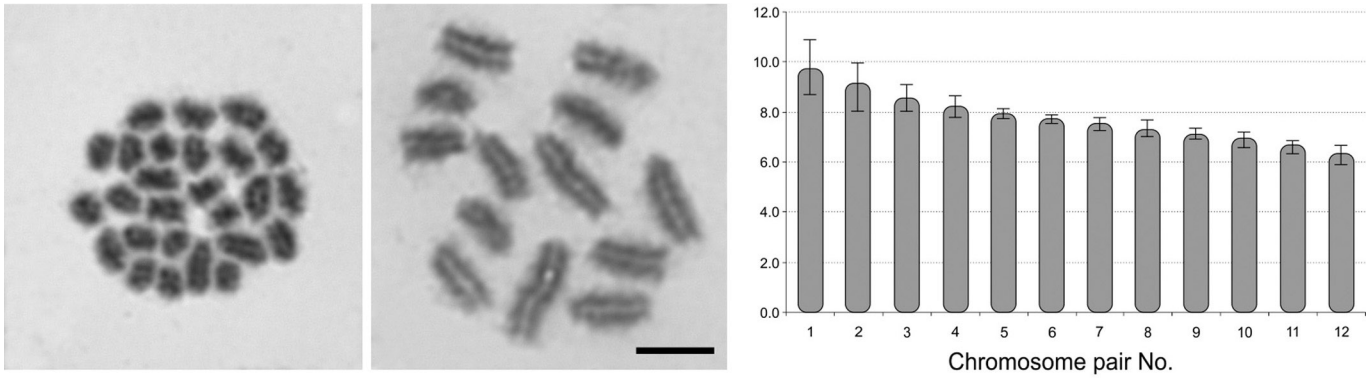

Figures 111–**113**: *Trypanothacus barnesi* **gen**. et **sp**. **n**., mitotic metaphase (111), postpachytene (112) and ideogram (113) (y axis - % of the chromosome length of the haploid set) of male holotype. Scale bar = 5 μm.

aculeus length/ vesicle length (the length of the aculeus integrated along its curve, normalized to vesicle length; cf. Fig. 107, inset, for measurements). Axes are logarithmic to account for allometric scaling. In this plot, the *Buthacus* data points are located towards the upper right (cyan symbols), and *Trypanothacus* **gen**. **n**. points more towards the lower left (dark blue symbols), showing that the latter indeed have more bulbous vesicles and shorter aculei. We wondered if these structural differences were linked to ecological and behavioral differences between the genera. Many members of *Buthacus* are known psammophiles that burrow in loose sand, whereas we found *T. barnesi* **sp**. **n**. inhabiting more compact, sedimentary soils of the Jiddat al-Harasis. Long term UV detection surveys in Oman by several collectors have not taken this species from psammophilous or ultrapsammophilous habitats such as the Rub' al-Khali (Empty Quarter) and Ramlat al-Wahiba (Wahiba/ Sharqiya sands). Adaptation to specific substrates is connected to certain scorpion morphologies, known as ecomorphotypes (Prendini, 2001). Psammophiles typically have strongly compressed basitarsi I–III, and both tibia and tarsi may bear dense series of long macrosetae (bristle-combs) (Fet et al., 1998). These modifications are present in many *Buthacus*, whereas in *Trypanothacus* **gen**. **n**., basitarsal compression and bristle-combs are more modestly developed. The metasoma of *Trypanothacus* **gen**. **n**. is fairly robust compared to many *Buthacus* species, with strong carination and enlarged ventral teeth on segments II–III and V (especially in females). Robust metasomal segments and sexually dimorphic, enlarged dentition on metasoma II–III and V, are features of other buthids that burrow in firmer soils (i.e., pelophilous or semi-psammophilous), e.g. *Buthus* Leach, 1815, *Odontobuthus* Vachon, 1950, *Femtobuthus* Lowe, 2010, and presumably *Pantobuthus* Lourenço & Duhem, 2009. To test whether telson shape is ecomorphotypic and correlated with substrate specialization, we included several other genera in the plot of Fig. 107, that are presumed or known as either psammophilous/ ultra-psammophilous (*Vachoniolus*: dark green symbols; *Apistobuthus* Finnegan, 1932, *Buthiscus* Birula, 1905, *Liobuthus* Birula, 1898, and *Plesiobuthus* Pocock, 1900: yellow symbols) or pelophilous/ semi-psammophilous (*Buthus*, *Odontobuthus*, *Pantobuthus*: orange symbols). Note that *Trypanothacus* **gen**. **n**. clusters with the pelophilous/ semi-psammophilous species, and is well separated from *Buthacus*, supporting its transfer to a different genus. The plotted genera and species were restricted to the Old World 'Buthus group', to focus on ecomorphotypic effects in a specific clade, and minimize phylogenetic or other influences in unrelated buthids and other scorpions, and also because most arenicolous buthids belong to this group (Fet et al., 1998). The data are taken from a class of larger body sizes (carapace L > ca. 4 mm) to avoid size scaling complications of very small scorpions (see below). In this set of large arenicolous 'Buthus group' scorpions, we obtained a positive correlation between vesicle elongation and aculeus length ($R = 0.57$, $p < 0.0001$; brown regression line), suggesting that ecomorphotypic factors play a role in telson shape.

We propose an ecological evolutionary model to explain these differences in aculeus length. We envisage a general positive selection pressure favoring a longer aculeus, as this will enable better penetration of thick layers of fur or feathers when a telson is employed as a defensive weapon to deliver vertebrate-specific neurotoxins, that are well known among 'Buthus group' scorpions, against mammalian or avian predators (Borges & Graham, 2014; Fet et al., 2003; Fet et al., 2005; Van der Meijden & Kleinteich, 2016). On the other hand, there may be negative selection pressures on aculeus length among species living in hard substrates. They can utilize their metasoma for scraping soil and stones during burrow excavation, and their strong metasomal carinae with lobate dentition would assist in this task. But a long, slender aculeus has mechanical weakness, being easier to break due to higher leverage forces (Van der Meijden & Kleinteich, 2016) if the metasoma were used as an earthmoving tool (Newlands, 1972a, 1972b), or as an anchor mechanism to brace the animal in its burrow (Lowe, 1993). Aculei with broken tips probably have severely curtailed venom delivery capability. A balance between these opposing selection pressures will limit the degree of aculeus extension in pelophilous or semi-psammophilous scorpions. Psammophilous and ultrapsammophilous species may be under less negative selection pressure, because aculeus impacts against soft sand are less likely to cause damage, and hence these scorpions can benefit from having

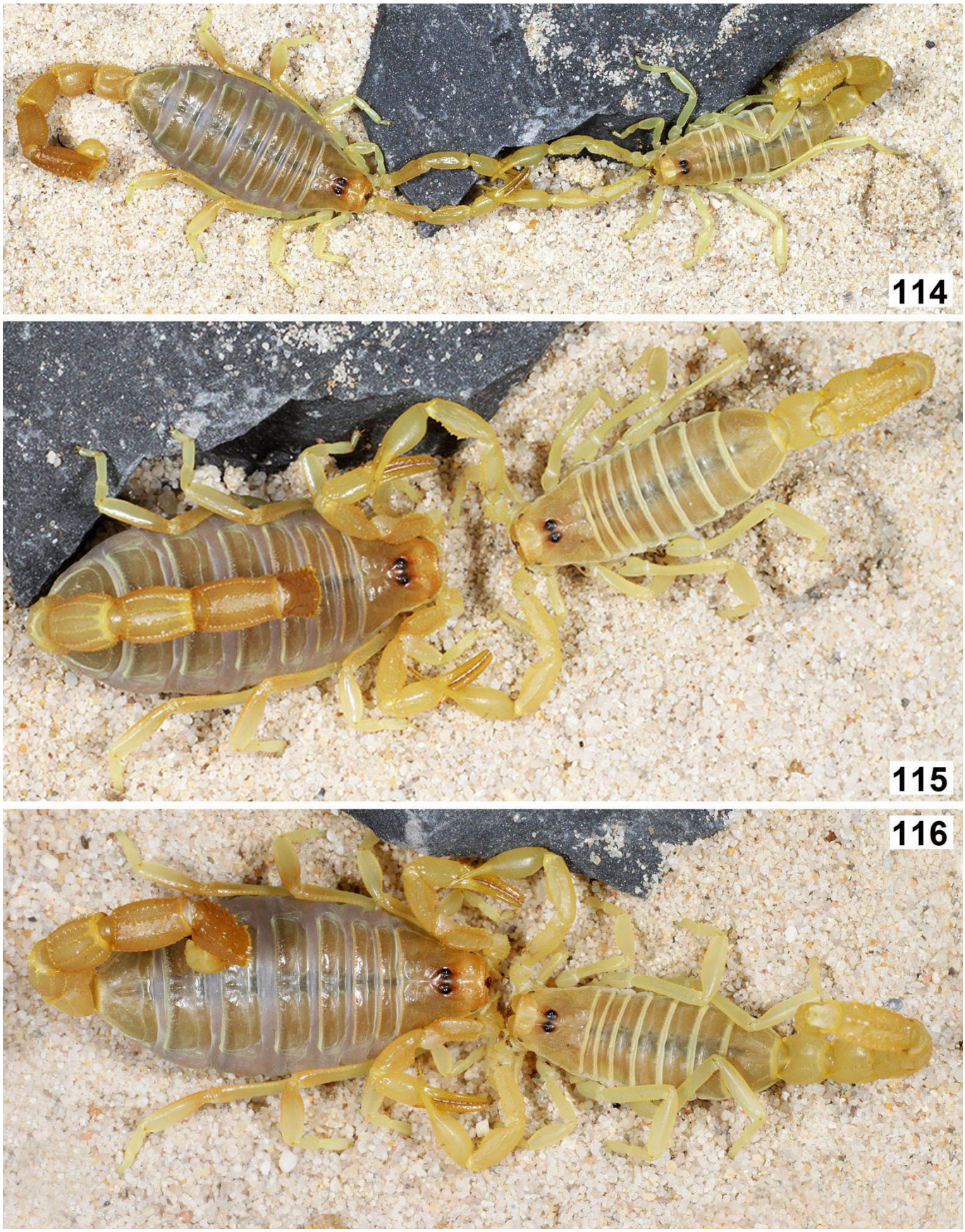

Figures 114–**116**: *Trypanothacus barnesi* **gen**. et **sp**. **n**., promenade à deux (courtship dance) in a mating pair of individuals collected from the type locality. Photos taken in laboratory. Male is on the right.

Figures 117–**118**: *Trypanothacus barnesi* **gen**. et **sp**. **n**., cheliceral massage (117) and spermatophore deposition (118) in a mating pair of individuals collected from the type locality. Photos taken in laboratory. Male is on the right.

longer aculei. This argument explains separation by substrate of points along the abscissa of Fig. 107, representing aculeus length. Along the ordinate, the less bulbous, more pyriform vesicle in psammophiles could be a result of aculeus extension requiring tapered posterior extension of the vesicle to act as a wider supporting base for a longer aculeus.

In Fig. 108, the positive correlation of Fig. 107 is shown in a wider context on a large scale plot including smaller (carapace L < ca. 4 mm) psammophile/ ultrapsammophile 'Buthus group' scorpions (in the genera: *Anomalobuthus* Kraepelin, 1901, *Compsobuthus* Vachon, 1949, *Lanzatus* Kovařík, 2001, *Neobuthus* Hirst, 1911, and *Picobuthus* Lowe, 2010: dark yellow symbols). The small sizes of these species are revealed in the plot of carapace length vs. relative aculeus length in Fig. 109. The small psammophiles deviate from the positive correlation trend of large species (i.e., from the brown line in Fig. 108). This implies a lack of positive selection pressure on aculeus length below a threshold body size. Our model of selection pressure may not apply to species that are too small to be able to sting through fur or feathers, and perhaps evolved other strategies to cope with predation by vertebrates. The background cloud of gray points in Fig. 108 represents a larger sample of known taxa (ca. 76%) in Order Scorpiones. The positive correlation for large 'Buthus group' species is seen to be embedded in an overall negative correlation of vesicle elongation vs. aculeus length for the whole order ($R = -0.62$, $p < 0.0001$, gray line). The average trend across all scorpions is that telsons with longer aculei are more bulbous, and those with shorter aculei are more elongated. Most plotted points in the upper left quadrant that cause this negative trend are non-buthids: bothriurids, chactids, chaerilids, diplocentrids, euscorpiids, hormurids, scorpionids, typhlochactids and vaejovids, which typically have an elongated vesicle and a short aculeus. In contrast to buthids, potent vertebrate-specific neurotoxins are not well known from these families.

The relationship between body size (using carapace length as a proxy) and aculeus length in Fig. 109 was well fit by linear regression ($R = 0.74$, $P < 0.0001$; blue line), i.e. among 'Buthus group' psammophiles, smaller species have a shorter aculeus and larger species a longer aculeus. In Fig. 110, this correlation is shown on a larger scale plot, where again Order Scorpiones is represented by gray background points. There was no correlation between body size and aculeus length over all scorpions ($R = -0.01$, $p = 0.50$; gray line). Once again, a positive correlation that exists in a specific subgroup of scorpions did not generalize to all scorpions. However, if attention is restricted to another subgroup, the species belonging to the largely psammophilous bothriurid genus, *Brachistosternus* Pocock, 1893 (Fig. 110, magenta symbols), we find another positive correlation of body size vs. aculeus length ($R = 0.39$, $p < 0.00027$, purple line). We also found that aculeus length was significantly correlated ($R = 0.40$, $p = 0.0012$, data not shown) with a numerical 'psammophily index' for *Brachistosternus* derived from anatomical metrics such as pigmentation and tarsal structures (Ojanguren-Affilastro et al., 2016). This is consistent with the trend in Fig. 107. These results suggest that some telson scaling laws can be generalized across ecologically and phylogenetically restricted subgroups of scorpions. In the context of our ecological model of selecting for aculeus elongation, *Brachistosternus* and other bothriurids are not known to possess potent vertebrate-specific toxins like the buthids, but they could still benefit from improved ability to sting mammals and birds if nociceptive actions via pain receptors contribute to predator deterrence (Rowe et al., 2013).

The fact that smaller local trends do not necessarily predict larger global trends probably reflects the complexity of factors determining telson shapes across diverse ecomorphotypic and taxonomic groups. The telson is a multifunctional organ, used not only for venom synthesis and delivery, but also serving functions in sensory physiology, pheromone production, mating behavior, and possibly other unknown purposes. Telson morphology may contain phylogenetic signal, but some care is needed to interpret and apply it in taxonomy.

Acknowledgments

We sincerely thank Patrick Schumacher and Britta Stockmann for their invaluable assistance and companionship during the field trips in Oman. Without their patience and efforts, this work would not be possible. We also thank Ambros Hänggi for loans of types of *Buthacus buettikeri* and other scorpions from Naturhistorisches Museum Basel (NHMB Nos. 1324, 2012020, 2012108). This work continues scorpion studies in Oman by the first author, originally sponsored by H. H. The Minister of National Heritage and Culture, Sultanate of Oman, with support from Khair Bin Antar Salim (Director of Museums), Said Ali Said Al-Farsi and Saddiqa Ramdhan, Ministry of National Heritage and Culture, and from Michael D. Gallagher, Oman Natural History Museum. The first author gratefully acknowledges advice, correspondence, photos in Figs. 86–87, and contributions of many Oman scorpion specimens of *Trypanothacus* **gen**. **n**. and other taxa from J. Neil Barnes. Also recognized are generous gifts from Victor Fet of buthid scorpions for comparative studies.

References

AHRENS, D. 2000. Sericinae (Coleoptera: Scarabaeoidea: Melolonthidae) of Arabia. *Fauna of Arabia*, 18: 177–210.

BIRULA, A. A. 1908. Ergebnisse der mit Subvention aus der Erbschaft Treitl unternommenen zoologischen Forschungsreise Dr. F. Werner`s nach dem ägyptischen Sudan und Nord-Uganda. XIV. Scorpiones und Solifugae. *Sitzungsberichte der Kaiserlich-Königlichen Akademie der Wissenschaften*, *Wien*, 117/2 (1): 121–152.

BORGES, A. & M. R. GRAHAM. Phylogenetics of scorpions of medical importance. Pp. 81–104 *in* GOPALAKRISHNAKONE, P. & J. J. CALVETE (Eds.) *Venom Genomics and Proteomics*. *Toxinology*. Springer, Dordrecht.

DESOUKY, M. M. A. & A. M. ALSHAMMARI. 2011. Scorpions of the Ha'il Region, northern Saudi Arabia, and molecular phylogenetics of two common species, *Androctonus crassicauda* and *Scorpio maurus kruglovi*. *Bulletin of the British Arachnological Society*, 15 (6): 193–200.

EL-HENNAWY, H. K. 2009. Scorpions of Saudi Arabia. *Serket*, 11 (3/4): 119–128.

EL-HENNAWY, H. K. 2014. Preliminary list of spiders and other arachnids of Saudi Arabia (Except ticks and mites). *Serket*, 14 (1): 22–58.

FET, V., B. GANTENBEIN, A. GROMOV, G. LOWE & W. R. LOURENÇO. 2003. The first molecular phylogeny of Buthidae (Scorpiones). *Euscorpius*, 4: 1–10.

FET, V., G. POLIS, & W. D. SISSOM. 1998. Life in sandy deserts: the scorpion model. *Journal of Arid Environments*. 39: 609–622.

FET, V., M. E. SOLEGLAD & G. LOWE. 2005. A new trichobothrial character for the high-level systematics of Buthoidea (Scorpiones: Buthida). *Euscorpius*, 23: 1–40.

HENDRIXSON, B. E. 2006. Buthid scorpions of Saudi Arabia, with notes on other families (Scorpiones: Buthidae, Liochelidae, Scorpionidae). *Fauna of Arabia*, 21: 33–120.

KOVAŘÍK, F. 2005. Taxonomic position of species of the genus *Buthacus* Birula, 1908 described by Ehrenberg and Lourenço, and description of a new species (Scorpiones: Buthidae). *Euscorpius*, 28: 1–13.

KOVAŘÍK, F. 2007. A revision of the genus *Hottentotta* Birula, 1908, with descriptions of four new species (Scorpiones, Buthidae). *Euscorpius*, 23: 1–40.

KOVAŘÍK, F. 2009. *Illustrated catalog of scorpions. Part I. Introductory remarks; keys to families and genera; subfamily Scorpioninae with keys to* Heterometrus *and* Pandinus *species.* Prague: Clairon Production, 170 pp.

KOVAŘÍK, F. 2018. Notes on the genera *Buthacus*, *Compsobuthus*, and *Lanzatus* with several synonymies and corrections of published characters (Scorpiones: Buthidae). *Euscorpius*, 269: 1–12.

KOVAŘÍK, F., G. LOWE, P. JUST, A. I. AWALE, H. SH A. ELMI & F. ŠŤÁHLAVSKÝ. 2018. Scorpions of the Horn of Africa (Arachnida: Scorpiones). Part XVI. Review of the genus *Gint* Kovařík et al., 2013, with description of three new species from Somaliland (Scorpiones, Buthidae). *Euscorpius*, 258: 1–41.

KOVAŘÍK,F.,G.LOWE,J.PLÍŠKOVÁ&F.ŠŤÁHLAVSKÝ. 2013. A new scorpion genus, *Gint* gen. n., from the Horn of Africa (Scorpiones, Buthidae). *Euscorpius*, 173: 1–19.

KOVAŘÍK, F., G. LOWE, K. B. RANAWANA, D. HOFEREK, V. A. SANJEEWA JAYARATHNE, J. PLÍŠKOVÁ & F. ŠŤÁHLAVSKÝ. 2016a. Scorpions of Sri Lanka (Arachnida, Scorpiones: Buthidae, Chaerilidae, Scorpionidae) with description of four new species of the genera *Charmus* Karsch, 1879 and *Reddyanus* Vachon, 1972 stat. n.. *Euscorpius*, 220: 1–133.

KOVAŘÍK, F., G. LOWE & F. ŠŤÁHLAVSKÝ. 2016b. Review of Northwestern African *Buthacus*, with description of *Buthacus stockmanni* sp. n. from Morocco and Western Sahara (Scorpiones, Buthidae). *Euscorpius*, 236: 1–18.

KOVAŘÍK, F. & A. A. OJANGUREN AFFILASTRO. 2013. *Illustrated catalog of scorpions Part II.* Bothriuridae; Chaerilidae; Buthidae I., genera *Compsobuthus*, *Hottentotta*, *Isometrus*, *Lychas*, and *Sassanidotus*. Prague: Clairon Production, 400 pp.

KOVAŘÍK,F.,F.ŠŤÁHLAVSKÝ.T.KOŘÍNKOVÁ,J.KRÁL & T. VAN DER ENDE. 2009. *Tityus ythieri* Lourenço, 2007 is a synonym of *Tityus magnimanus* Pocock, 1897 (Scorpiones: Buthidae): a combined approach using morphology, hybridization experiments, chromosomes, and mitochondrial DNA. *Euscorpius*, 77: 1–12.

LEVY, G. & P. AMITAI. 1980. *Scorpiones*. *Fauna Palaestina. Arachnida* I. The Israel Academy of Sciences and Humanities. Jerusalem, 1980.

LEVY, G., P. AMITAI & A. SHULOV. 1973. New scorpions from Israel, Jordan and Arabia. *Zoological Journal of the Linnean Society*, 52 (2): 113–140.

LEWIS, D. J. & W. BÜTTIKER. 1982. Insects of Saudi Arabia. The taxonomy and distribution of Saudi Arabian phlebotomine sandflies (Diptera: Psychodidae). *Fauna of Saudi Arabia*, 4: 353–397.

LORIA, S. F. & L. PRENDINI. 2014. Homology of the lateral eyes of Scorpiones: a six-ocellus model. *PLoS ONE* 9(12): e112913. doi:10.1371/journal.pone.0112913.

LOURENÇO, W. R. 2006. Further considerations on the genus *Buthacus* Birula, 1908 (Scorpiones: Buthidae), with a description of one new species and two new subspecies. *Boletín de la Sociedad Entomológica Aragonesa*, 38: 59–70.

LOURENÇO, W. R. & E.-A. LEGUIN. 2009. A new species of the genus *Buthacus* Birula, 1908 from the United Arab Emirates (Scorpiones, Buthidae). *Zoology in the Middle East*, 46: 103–108.

LOURENÇO, W. R. & J-X. QI. 2006. A new species of the genus *Buthacus* Birula, 1908 (Scorpiones, Buthidae), from Pakistan. *Boletín de la Sociedad Entomológica Aragonesa*, 39: 161–164.

LOWE, G. 1993. Tales of tails: scorpions in Oman. *The Historical Association of Oman. Newsltter. Natural History*. No. 2.

LOWE, G. 2010a. A new species of *Odontobuthus* (Scorpiones: Buthidae) from northern Oman. *Euscorpius*, 96: 1–22.

LOWE, G. 2010b. The genus *Vachoniolus* (Scorpiones: Buthidae) in Oman. *Euscorpius*, 100: 1–37.

LOWE, G. 2018. The genera *Butheolus* Simon, 1882 and *Xenobuthus* gen. nov. (Scorpiones: Buthidae) in Oman. *Euscorpius*, 261: 1–73.

LOWE, G., E. A. YAĞMUR & F. KOVAŘÍK. 2014. A review of the genus *Leiurus* Ehrenberg, 1828 (Scorpiones: Buthidae) with description of four new species from the Arabian Peninsula. *Euscorpius*, 100: 1–37.

MATTOS, V. F., D. M. CELLA, L. S. CARVALHO, D. M. CANDIDO&M.C.SCHNEIDER.2013.Highchromosome variability and the presence of multivalent associations in buthid scorpions. *Chromosome Research*, 21: 121–136.

NEWLANDS, G. 1972a. Notes on psammophilous scorpions and description of a new species (Arachnida: Scorpionides). *Annals of the Transvaal Museum*, 27 (12): 241–254.

NEWLANDS, G. 1972b. Ecological adaptations of Kruger National Park scorpionids (Arachnida: Scorpionides). *Koedoe*, 15: 37–48.

OJANGUREN-AFFILASTRO, A. A., C. I. MATTONI, J. A. OCHOA, M. J. RAMÍREZ, F. S. CECCARELLI & L. PRENDINI. 2016. Phylogeny, species delimitation and convergence in the South American bothriurid scorpion genus *Brachistosternus* Pocock 1893: Integrating morphology, nuclear and mitochondrial DNA. *Molecular Phylogenetics and Evolution*, 94: 159–170.

PRENDINI, L. 2001. Substratum specialization and speciation in southern African scorpions: the effect hypothesis revisited. Pp. 113–138 in: Fet, V & Selden, P.A. (eds). *Scorpions 2001. In Memoriam Gary A. Polis*. Burnham Beeches, Bucks. British Arachnological Society.

ROWE, A.H., Y. XIAO, M. ROWE, T. CUMMINS & H. ZAKON. 2013. Voltage-gated sodium channel in grasshopper mice defends against bark scorpion toxin. *Science*, 342: 441–447.

SIMON, E. 1892. Liste des arachnides recueillis en Syrie par M. le docteur Théod. Barrois. *Revue Biologique du Nord de la France*, 5: 80–84.

SISSOM, W. D. 1990. Systematics, biogeography and paleontology. Pp. 64–160 *in* POLIS, G. A. (Ed.) *The Biology of Scorpions*. Stanford University Press, Stanford, California.

SISSOM, W. D., G. A. POLIS & D. D. WATT. 1990. Field and laboratory methods. Pp. 445–461 *in* POLIS, G. A. (ed.). *The Biology of Scorpions*. Stanford University Press, Stanford, CA.

STAHNKE, H. L. 1971. Scorpion nomenclature and mensuration. *Entomological News*, 81: 297–316.

VACHON, M. 1949. Études sur les Scorpions. III (suite). Déscription des Scorpions du Nord de l'Afrique. *Archives de l'Institut Pasteur d'Algérie*, 27(1): 66–100.

VACHON, M. 1952. *Étude sur les Scorpions*. Institut Pasteur d'Algérie, Alger, 482 pp.

VACHON, M. 1953. Contribution à'l étude du peuplement de la Mauritanie. Scorpions. *Bulletin d'Institut Français d'Afrique Noire*, 55(3): 1012–1028.

VACHON, M. 1963. De l'utilité, en systématique, d'une nomenclature des dents de chélicères chez les scorpions. *Bulletin du Musèum National d'Histoire Naturelle, Paris*, (2), 35 (2): 161–166.

VACHON, M. 1974. Études des caractères utilisés pour classer les familles et les genres des scorpions (Arachnides). 1. La trichobothriotaxie en arachnologie. Sigles trichobothriaux et types de trichobothriotaxie chez les Scorpions. *Bulletin du Muséum national d'Histoire naturelle*, 3e série, 140 (Zoologie, 104): 857–958.

VACHON, M. 1975. Sur l'utilisation de la trichobothriotaxie du bras des pedipalps des Scorpions (Arachnides) dans le classement des genres de famille des Buthidae Simon. *Compte rendus hebdomadaires des séances de l'Academie des Sciences, Paris Ser.D Sciences Naturelles*, 281 (21): 1597–1599.

VACHON, M. 1979. Arachnids of Saudi Arabia, Scorpiones. *Fauna of Saudi Arabia*, 1: 30–66.

VAN DER MEIJDEN, A. & T. KLEINTEICH. 2016. A biomechanical view on stinger diversity in scorpions. *Journal of Anatomy*, 230(4): 497–509.